

March 20, 2019

ACP Editor

Dear Prof. Nga Lee Ng,

Enclosed please find our revised manuscript entitled “*Partitioning of hydrogen peroxide in gas-liquid and gas-aerosol phases*”, revised supplement and two responses to the anonymous referees #1 and #2, respectively. We gratefully thank the reviewers for their constructive suggestions that help us to improve the manuscript. Detailed, point-by-point responses to the comments and corresponding revisions to the manuscript and supplement have been submitted. We sincerely hope that this revised manuscript will be finally acceptable to be published on ACP.

The major revisions are specified as follows:

1. We have reevaluated the sources and sinks of aerosol-phase H_2O_2 based on the formation and consumption rates according to the reviewers' suggestions, and adjusted Table 3 and 4 in the revised manuscript. The ratios of contributions from different pathways have also been modified accordingly.
2. We have calculated the effective Henry's law constant from 2 Jan to 3 Jan 2019 and the contribution of heterogeneous uptake of HO_2 to the aerosol-phase H_2O_2 .
3. We have discussed the influence of the “salting-in” effect on the aerosol-phase H_2O_2 .
4. We have added some descriptions to prove the validity of the current technique of studying the gas-aerosol partitioning of H_2O_2 .
5. We have added the experimental conditions of the extracted solution and proved that the derived rates of decomposition can be applied to the ambient atmosphere.
6. We have clarified some numbers (e.g., 88%, 86% and 0.5%), the collection efficiency of organic peroxides, and gas-phase H_2O_2 concentration used to estimate the liquid-phase H_2O_2 .
7. We have explained the reasons for using $8.4 \times 10^4 \text{ M atm}^{-1}$ as Henry's law constant, using the $\text{PM}_{2.5}$ concentration as an indicator to calculate the effective gas-aerosol partitioning, the inverse relationship between H_2O_2 level and $\text{PM}_{2.5}$ /sulfate levels, and whether rain samples follow Henry's law.
8. We have corrected the language and grammar errors of the previous manuscript.
9. We have resized Figures 1–6.

The data corrections are specified as follows:

1. The aerosol surface area and the gas-phase H_2O_2 level in the previous manuscript were calculated incorrectly. We have revised them in Table 3 and reevaluated the contribution of heterogeneous uptake of H_2O_2 to the aerosol-phase H_2O_2 .

Detailed changes made in the revised manuscript can be seen in the marked-up version in this response.

Thanks for your time.

Sincerely yours,

Zhongming Chen and co-authors

Response to Reviewer #1

We gratefully thank you for your constructive comments and thorough review. Our point-by-point responses can be found below.

(Q=Question, A=Answer, C=Change in the revised manuscript)

General comments:

Q1: Xuan et al. performed field measurements of the gas-, liquid- and aerosol-phase H_2O_2 in the urban atmosphere of Beijing to understand the partitioning of H_2O_2 between gas- and liquid-phase or aerosol-phase. They show that the partitioning of H_2O_2 in the gas-liquid phase can be explained by Henry's law and the residual H_2O_2 in the raindrops while the aerosol-phase H_2O_2 level is significantly higher than that predicted value based on Pankow's absorptive partitioning theory. This paper has important implications for understanding the H_2O_2 chemistry and sulfate formation in the atmosphere, so it is well within the scope of ACP. This paper is of great interest to the atmospheric community although some clarifications regarding the data analysis are required. I recommend this paper to be published after addressing the specific comments below.

A1: We highly appreciate your comments and suggestions. The questions you mentioned are specifically answered as follows.

Specific comments:

Q2. Estimation of effective partitioning coefficients: The authors determined the gas-aerosol partitioning coefficient instead of the effective Henry's law constant for the gas-aerosol phase. Is this due to that aerosol water content cannot be accurately estimated for low RH? The effective Henry's law constant should be estimated for the high RH condition, e.g. heavy haze episodes from 2 Jan to 3 Jan 2019 and compared with the theoretical value.

A2: Yes, you are right. After considering your suggestion, we have calculated the effective Henry's law constant for the gas-aerosol phase during a heavy haze episode from 2 Jan to 3 Jan 2019 and compared it with the theoretical value in the revised manuscript.

C2: Lines 267–272 in Sec. 3.2.1:

“Because aerosol water content (AWC) cannot be correctly evaluated at low RH, the effective field-derived Henry's law constant (H_p^m) of H_2O_2 was estimated for high RH condition, e.g. a heavy haze episode from 2 January to 3 January 2019 (RH, 30 %). Details regarding the estimation of AWC was shown in the Supplement. It was calculated that AWC, C_p^m and C_g^m levels averaged $3.20 \mu\text{g m}^{-3}$, $6.63 \times 10^3 \mu\text{M}$, and $1.90 \times 10^{-11} \text{ atm}$. Based on Eq. (5), the average H_p^m on 2–3 January 2019 was calculated to be $2.7 \times 10^8 \pm 1.8 \times 10^8 \text{ M atm}^{-1}$. However, the theoretical Henry's law constant (H_p^t) at 270 K was $1.1 \times 10^6 \text{ M atm}^{-1}$ (Sander et al., 2011), which was lower than H_p^m by two orders of magnitude.”

Q3. The authors estimated that heterogeneous uptake of H_2O_2 could account for 86% of the measured H_2O_2 in the aerosol phase in Sec 3.2.3 while stated that the heterogeneous uptake of H_2O_2 on aerosols contributed less than 0.5% of the aerosol-phase H_2O_2 in Sec 3.3. Please clarify.

A3: Thanks for your advice. The two percentages are calculated in different methods. 86 % refers to the ratio of the amount of heterogeneous uptake of H_2O_2 to the measured aerosol-phase H_2O_2 level, while 0.5 % refers to the ratio of the amount of heterogeneous uptake of H_2O_2 to the consumption amount of aerosol-phase H_2O_2 . In addition, we have reevaluated the contribution of the heterogeneous uptake to the aerosol-phase H_2O_2 based on the formation and consumption rates according to the reviewers' suggestions, and the heterogeneous uptake could account for 2 % of the consumption rate of the aerosol-phase H_2O_2 . To avoid confusion, we have removed 86 % in Sec. 3.2.3 and 0.5 % in Sec. 3.3.

Q4. The authors stated that the rates of the decomposition/hydrolysis of organic peroxides in the first and second types were $0.14 \text{ ng } \mu\text{g}^{-1}$ and $3.65 \text{ ng } \mu\text{g}^{-1}$ (lines 296–297) and further estimated the contribution of decomposition/hydrolysis of organic peroxides to aerosol H_2O_2 to be 32% (lines 343–346). However, these numbers seem to be the steady-state or maximum amount of H_2O_2 , not formation rates. The estimation should be based on the formation and consumption rate of H_2O_2 .

A4: Thanks for your suggestion. We have recalculated the estimation considering the formation and consumption rates of H_2O_2 and removed the calculation based on the steady-state or maximum amount of H_2O_2 in the revised manuscript. Furthermore, we have changed the relevant data in Table 3 and 4.

C4: Lines 417–430 in Sec. 3.3:

“We estimated the contribution of different sources to the aerosol-phase H_2O_2 based on the formation and consumption rates. According to the previous estimation of the theoretical sulfate formation rate from January 2 to January 3 2019 ($0.29 \text{ } \mu\text{g m}^{-3} \text{ h}^{-1}$) and the average mass concentration of $\text{PM}_{2.5}$ ($106.19 \text{ } \mu\text{g m}^{-3}$), the consumption rate of H_2O_2 should be $0.97 \text{ ng } \mu\text{g}^{-1} \text{ h}^{-1}$. With respect to the sources of the aerosol-phase H_2O_2 , the decomposition/hydrolysis of organic peroxides was firstly considered, with average rates of the rising stage for the first and second types (Fig. 6), $0.01 \text{ ng } \mu\text{g}^{-1} \text{ h}^{-1}$ and $0.10 \text{ ng } \mu\text{g}^{-1} \text{ h}^{-1}$, respectively. Because the extracted solution was stored under 255 K, lower than the actual atmospheric temperature (270 K), the decomposition/hydrolysis rates of organic peroxides were underestimated and an adjusting factor should be multiplied. The factors for the three typical labile organic peroxides (HMHP, PFA, and PAA) were 13, 3, and 2, respectively, as shown in the Supplement. Assuming the factor was in the range of 2–13, the average decomposition/hydrolysis rate of organic peroxides for the first and second types ($0.055 \text{ ng } \mu\text{g}^{-1} \text{ h}^{-1}$) was used to calculate the formation rate. The formation rate of the aerosol-phase H_2O_2 from the decomposition/hydrolysis of organic peroxides could account for 11–74 % of the consumption rate by sulfate formation. Moreover, the heterogeneous uptake of HO_2 and H_2O_2 were also likely to improve the aerosol-phase H_2O_2 level at the rates of $0.22 \text{ ng } \mu\text{g}^{-1} \text{ h}^{-1}$ and $0.02 \text{ ng } \mu\text{g}^{-1} \text{ h}^{-1}$, respectively, which can offset 22 % and 2 % of the consumption rate of H_2O_2 , respectively.”

Q5. Though the heterogeneous uptake of HO_2 on aerosols is not well understood, it is possible to estimate its contribution to aerosol H_2O_2 using the reactive uptake coefficient of HO_2 to aerosol from literature and assuming the product to be H_2O_2 (Li et al., 2019). It is recommended to perform such calculations to provide more insights.

A5: Thanks for your advice. We have added the calculation of the heterogeneous uptake of HO_2 on

aerosols in the revised manuscript.

C5: Lines 325–331 in Sec. 3.2.3:

“As HO₂ radical is a precursor of H₂O₂, the heterogeneous uptake of HO₂ onto aerosols may also contribute to the formation of the aerosol-phase H₂O₂. We assumed that the reactive uptake coefficient of HO₂ to aerosol particles was 0.2, and the product of HO₂ was H₂O₂ (Li et al., 2019). At the same observation site in winter of 2017, HO₂ concentration for noontime averaged $(0.4 \pm 0.2) \times 10^8 \text{ cm}^{-3}$ and $(0.3 \pm 0.2) \times 10^8 \text{ cm}^{-3}$ on clean and polluted days, respectively (Ma et al., 2019). Since HO₂ level data in 2018 was not available, we used the level of HO₂ on clean days in winter of 2017 for calculations, and the average was about $0.2 \times 10^8 \text{ cm}^{-3}$ at day-time. The heterogenous uptake rate of HO₂ on aerosols was calculated the same way as H₂O₂, and the formation rate of the aerosol-phase H₂O₂ by reactive uptake of HO₂ averaged $0.22 \text{ ng } \mu\text{g}^{-1} \text{ h}^{-1}$ at all day.”

Q6. The authors should discuss the “salting in” effect of high ionic strength of aerosol particles on gas-aerosol partitioning of H₂O₂ though it may only have a minor contribution to the enhanced aerosol H₂O₂ concentrations.

A6: Thanks for your suggestion. We have discussed the “salting-in” effect of high ionic strength of aerosol particles on the gas-aerosol partitioning of H₂O₂ in the revised manuscript.

C6: Lines 272–278 in Sec. 3.2.1:

“In Chung’s study (2005), “salting-in” effect can improve the level of H₂O₂ by a factor of two when the concentrations in salt solutions were up to 10 M, and the most obvious “salting-in” effect of salt solutions was ammonium sulfate. In this paper, the levels of aerosol-phase NH₄⁺ and SO₄²⁻ on 2–3 January 2019 were 94 M and 21 M, respectively, and the level of (NH₄)₂SO₄ was assumed to be 21 M. The increasement of H_p^m by the “salting-in” effect of (NH₄)₂SO₄ was about $3.2 \times 10^6 \text{ M atm}^{-1}$ at 286 K based on equations in Chung et al. (2005). Even though aerosol particles were collected at $270 \pm 4 \text{ K}$ and the increasement may be greater, the “salting-in” effect could not fully explain the difference between H_p^m and H_p^f . Other sources need to be found later.”

Q7. Line 82: Are the organic peroxide concentrations corrected for the collection efficiency?

A7: Thanks for your suggestion. Because the measured concentrations of organic peroxides were near the detection limit of the HPLC method in BJ-2018 Winter measurement, the levels of organic peroxides were not discussed in this paper. Alternatively, we used the concept of total peroxides as a measure to estimate the sources of the aerosol-phase H₂O₂ in Sec. 3.2. The level of total peroxides was measured using the iodometric spectrophotometric method with an extraction efficiency close to ~ 98 % (Li et al., 2016), so we did not correct the total peroxides level.

Q8. Lines 149–150: Please explain how 88% is derived.

A8: Thanks for your suggestion and we have explained it in line 166 in the revised manuscript. The percentage was calculated as the average ratio of the predicted level to measured level of H₂O₂ in each rain sample. The value indicated that 88 % of the liquid-phase H₂O₂ in all the rain samples collected was from gas-phase partitioning. Since the measured H₂O₂ level in some rain samples was lower than the

predicted value, gas-phase partitioning accounted for a high proportion in all samples based on statistics on averages.

Q9. Line 181: What is the gas-phase H_2O_2 concentration used to estimate the liquid-phase H_2O_2 ?

A9: The gas-phase H_2O_2 concentration used to estimate the liquid-phase H_2O_2 was 0.30 ± 0.26 ppbv, and we have added it in lines 203–204 in the revised manuscript. We assumed that the gas-phase H_2O_2 concentration was homogeneous, and the gas-phase H_2O_2 in the cloud atmosphere was equal to the gas-phase H_2O_2 near the ground (line 191).

Q10. Section 3.2.4: The experimental details on the decomposition of organic peroxides should be provided. Is the extracted solution exposed to light at room temperature? Are these experiments conducted at atmospheric relevant conditions so that the derived rates of decomposition can be applied to ambient?

A10: Thanks for your suggestion. The extracted solution was away from light at 255 K. The experimental conditions were chosen based on certain considerations, which have been added in the revised manuscript and Supplement. The influence of experimental conditions on the derived rates has also been discussed in the revised manuscript and Supplement. We think that the derived rates of decomposition can be applied to the ambient atmosphere.

C10: Lines 111–115 in Sec. 2.2.3:

“The remaining extracted solution was stored at 255 K away from light for subsequent measurement of H_2O_2 concentration variation with time, and details of the experimental conditions of the extracted solution are shown in the Supplement. Photochemical reactions of aerosols may produce aerosol-phase H_2O_2 (Zhou et al., 2008), and the effect of the photochemical reactions on the level of H_2O_2 in the extracted solution was discussed in the Supplement.”

Lines 1–48 in the Supplement:

“The extracted solution was stored under refrigeration at 255 K, away from light. The first reason to choose 255 K was that the temperature during BJ-2018 Winter measurement averaged 270 K, less than 273 K. The second reason was that under 255 K, the decomposition rate of H_2O_2 should be reduced, which contributed to a more accurate estimation of the decomposition rates of organic peroxides to H_2O_2 . Li et al. (2016) studied the stability of H_2O_2 in SOA stored on-filter at 255 K and 298 K. It was found that the level of H_2O_2 remained stable for 6 days at 255 K but decreased gradually at 298 K. The third reason was that the H_2O_2 level in the extracted solution was very low at time=0, which could easily decompose at 277 K, therefore, the extracted solution should be stored at 255 K.

Due to the positive correlation between temperature and decomposition rates, the derived rates of decomposition in this paper were lower than the actual rates of decomposition. To discuss the influence of the storage temperature on the decomposition rates of organic peroxides, hydroxymethyl hydroperoxide (HMHP), peroxyformic acid (PFA), and peroxyacetic acid (PAA) were chosen as representatives. According to the Arrhenius equation, the reaction rate usually increases exponentially as temperature increases. The ratios of the decomposition/hydrolysis rates of HMHP, PFA, and PAA at 270 K to 255 K were 13, 3, and 2, respectively (Zhou and Lee, 1992; Dul’neva and Moskvina, 2005; Sun et

al., 2011). We have considered the influence of temperature on the decomposition rates of organic peroxides when calculating the aerosol-phase H_2O_2 formation rate from the decomposition/hydrolysis of organic peroxides, as shown in Sec. 3.3.

The extracted solution was away from light in this paper, which was different from atmospheric relevant conditions (i.e., exposure to sunlight in the ambient atmosphere), and may affect the data applicability in this study. We chose this experimental condition because if the extracted solution was exposed to sunlight, the photochemical reactions of organic matters and the decomposition/hydrolysis of organic peroxides will coexist, and we cannot distinguish the effects of these two processes. By doing so, the specific contribution of the decomposition/hydrolysis of organic peroxides to the aerosol-phase H_2O_2 was estimated. With respect to the photochemical reactions of organic matters, Zhou et al. (2008) have discussed that as the exposure time of the extracted solution to sunlight increased, the production of peroxides in nascent marine aerosols first increased rapidly and then slowly. The change trend in Zhou's study was the same as that of the aerosol-phase H_2O_2 level in this paper (Fig. 6). The estimated 24-h-average rate of H_2O_2 photochemical production in Alert particles was about 9 mM h^{-1} at 248 K (Anastasio and Jordan, 2004). We assumed that the photoformation rate of H_2O_2 in Beijing particles was also 9 mM h^{-1} . And the concentrations of AWC and $\text{PM}_{2.5}$ from 2 January to 3 January 2019 were $3.20 \text{ } \mu\text{g m}^{-3}$ and $90.36 \text{ } \mu\text{g m}^{-3}$, respectively. The formation rate of the aerosol-phase H_2O_2 from photochemical reactions was estimated to be $0.011 \text{ ng } \mu\text{g}^{-1} \text{ h}^{-1}$ at 248 K. In addition, the activation energy of H_2O_2 photoformation was 9 kJ mol^{-1} (Anastasio et al., 1994), and the rate of H_2O_2 photoformation at 270 K should be 1.4 times higher than the value at 248 K. Compared with the aerosol-phase H_2O_2 formation rates from the decomposition/hydrolysis of organic peroxides and the heterogeneous uptake of HO_2 , the H_2O_2 photoformation could be neglected.

Based on the above analysis, we believe that the derived rates of decomposition under the experimental conditions in this paper can be applied to the ambient atmosphere.”

Technical corrections:

Q11. Lines 59–60: References are missing.

A11: Thanks for your reminder. We have added related references in line 65.

Q12. Equation 4: TSP or $\text{PM}_{2.5}$ should be used instead of C_{om} .

A12: Yes, we have changed “ C_{om} ” into “TSP” in Eq. (4) in the revised manuscript, and used the $\text{PM}_{2.5}$ mass concentration as an indicator because the $\text{PM}_{2.5}$ concentration was available based on our measurements.

Q13. Line 331: “measured” should be “was measured to be”.

A13: Thanks for your advice. We have revised it in line 391.

References

Anastasio, C., Faust, B. C., and Allen, J. M.: Aqueous phase photochemical formation of hydrogen peroxide in authentic cloud waters, *J. Geophys. Res.*, 99, 8231–8248,

- <https://doi.org/10.1029/94JD00085>, 1994.
- Anastasio, C., and Jordan, A. L.: Photoformation of hydroxyl radical and hydrogen peroxide in aerosol particles from Alert, Nunavut: implications for aerosol and snowpack chemistry in the Arctic, *Atmos. Environ.*, 38, 1153–1166, <https://doi.org/10.1016/j.atmosenv.2003.11.016>, 2004.
- Chung, M. Y., Muthana, S., Paluyo, R. N., and Hasson, A. S.: Measurements of effective Henry's law constants for hydrogen peroxide in concentrated salt solutions, *Atmos. Environ.*, 39, 2981–2989, <https://doi.org/10.1016/j.atmosenv.2005.01.025>, 2005.
- Dul'neva, L. V. and Moskvina, A. V.: Kinetics of formation of peroxyacetic acid, *Russ. J. Gen. Chem.*, 75, 1125–1130, <https://doi.org/10.1007/s11176-005-0378-8>, 2005.
- Kuang, Y., Tao, J. C., Xu, W. Y., Yu, Y. L., Zhao, G., Shen, C. Y., Bian, Y. X., and Zhao, C. S.: Calculating ambient aerosol surface area concentrations using aerosol light scattering enhancement measurements, *Atmos. Environ.*, 216, 116919, <https://doi.org/10.1016/j.atmosenv.2019.116919>, 2019.
- Li, H., Chen, Z. M., Huang, L. B., and Huang, D.: Organic peroxides' gas-particle partitioning and rapid heterogeneous decomposition on secondary organic aerosol, *Atmos. Chem. Phys.*, 16, 1837–1848, <https://doi.org/10.5194/acp-16-1837-2016>, 2016.
- Li, K., Jacob, D. J., Liao, H., Zhu, J., Shah, V., Shen, L., Bates, K. H., Zhang, Q., and Zhai, S. X.: A two-pollutant strategy for improving ozone and particulate air quality in China, *Nat. Geosci.*, 12, 906–910, <https://doi.org/10.1038/s41561-019-0464-x>, 2019.
- Ma, X. F., Tan, Z. F., Lu, K. D., Yang, X. P., Liu, Y. H., Li, S. L., Li, X., Chen, S. Y., Novelli, A., Cho, C. M., Zeng, L. M., Wahner, A., and Zhang, Y. H.: Winter photochemistry in Beijing: observation and model simulation of OH and HO₂ radicals at an urban site, *Sci. Total Environ.*, 685, 85–95, <https://doi.org/10.1016/j.scitotenv.2019.05.329>, 2019.
- Sander, S. P., Abbatt, J., Barker, J. R., Burkholder, J. B., Friedl, R. R., Golden, D. M., Huie, R. E., Kolb, C. E., Kurylo, M. J., Moortgat, G. K., Orkin, V. L., and Wine, P. H.: Chemical kinetics and photochemical data for use in atmospheric studies, Evaluation No. 17, JPL Publication 10-6, Jet Propulsion Laboratory, Pasadena, <http://jpldataeval.jpl.nasa.gov> (last access: 19 March 2020), 2011.
- Sun, X. Y., Zhao, X. B., Du, W., and Liu, D. H.: Kinetics of formic acid-autocatalyzed preparation of performic acid in aqueous phase, *Chin. J. Chem. Eng.*, 19, 964–971, [https://doi.org/10.1016/S1004-9541\(11\)60078-5](https://doi.org/10.1016/S1004-9541(11)60078-5), 2011.
- Wu, Q. Q., Huang, L. B., Liang, H., Zhao, Y., Huang, D., and Chen, Z. M.: Heterogeneous reaction of peroxyacetic acid and hydrogen peroxide on ambient aerosol particles under dry and humid conditions: kinetics, mechanism and implications, *Atmos. Chem. Phys.*, 15, 6851–6866, <https://doi.org/10.5194/acp-15-6851-2015>, 2015.
- Zhou, X. L., Davis, A. J., Kieber, D. J., Keene, W. C., Maben, J. R., Maring, H., Dahl, E. E., Izaguirre, M. A., Sander, R., and Smeyd-Weinstein, L.: Photochemical production of hydroxyl radical and hydroperoxides in water extracts of nascent marine aerosols produced by bursting bubbles from Sargasso seawater, *Geophys. Res. Lett.*, 35, L20803, <https://doi.org/10.1029/2008GL035418>, 2008.
- Zhou, X. L., and Lee, Y. N.: Aqueous solubility and reaction kinetics of hydroxymethyl hydroperoxide, *J. Phys. Chem.*, 96, 265–272, <https://doi.org/10.1021/j100180a051>, 1992.

Table 3: Calculating the theoretical heterogeneous uptake rate of H₂O₂ on aerosols ($d[X]_p^{t,h}/dt$)^a.

Parameters	T_W (K)	RH (%)	γ — ^b	S_{aw} (cm ²) ^c	$[X]_g$ (molecules m ⁻³) ^d	$d[X]_p^{t,h}/dt$ (ng μg^{-1} h ⁻¹)
Averages	270	17.89	1.54×10^{-4}	46	6.54×10^{14}	0.02

^a These parameters are calculated based on Wu et al. (2015).

^b γ is the heterogeneous uptake coefficient, dimensionless.

^c S_{aw} is the surface area of aerosols, quoted from Kuang et al. (2019).

^d $[X]_g$ is the concentration of gas-phase H₂O₂.

Table 4: Comparison of the H₂O₂ evolution parameters in the extracted solution among the three types.

Parameters	First type	Second type	Third type
Peak time (h)	5	40	–
Decomposition rate of organic peroxides to H ₂ O ₂ (ng μg ⁻¹ h ⁻¹)	0.01	0.10	–
C_{max}/C_0 of H ₂ O ₂ (μM/μM)	1.52	39.22	1.00
TPOs/H ₂ O ₂ (μM/μM)	5.25	40.06	47.59
Ratio of decomposable organic peroxides (%)	29	98	0

Response to Reviewer #2

We gratefully thank you for your constructive comments and thorough review. Our point-by-point responses can be found below.

(Q=Question, A=Answer, C=Change in the revised manuscript)

Q1: This manuscript by Xuan et al describes a detailed study of the partitioning of H_2O_2 in the atmosphere through field measurements. The authors quantified H_2O_2 in the gas phase, aerosol, and rainwater (as a surrogate for cloud water). By comparing the measured and theoretical Henry's law constant, as well as the measured and theoretical partitioning coefficient, the authors conclude that the measured values for both are higher than the theoretical values. An in-depth assessment is conducted to evaluate the influence of raindrop falling on the quantified H_2O_2 concentration, as well, a discussion on the source and sink of H_2O_2 in aerosol is provided. H_2O_2 plays an important role in the atmosphere, and understanding its partitioning in different atmospheric phases is of great importance for the atmospheric chemistry community. The manuscript is within the scope of ACP. The data analysis and calculation were performed with caution. I recommend publication on ACP after addressing the following comments.

A1: We highly appreciate your comments and suggestions. The questions you mentioned are specifically answered as follows.

Major comment:

Q2. In section 3.2.4, the authors present the evolution of H_2O_2 as a function of time in the aerosol abstract, and a detailed discussion on the potential source of H_2O_2 . This result highlights the challenges in making off-line H_2O_2 measurement from filter samples. Especially, when the sampling time is as long as 11.5 h (Line 100), it is very likely that the organic peroxides present in the aerosol sample is continuously decomposing on the filter. The authors categorize the H_2O_2 evolution into three types and postulate the relevant source of H_2O_2 for each type. However, in my opinion, this appears too speculative. The decomposition of H_2O_2 on filter is difficult to control, and the quantified H_2O_2 could be merely a snapshot of an ongoing decomposition process. The authors must justify whether it is valid at all to establish gas-aerosol partitioning of H_2O_2 based on the current technique.

A2: Thanks for your suggestion. We have deleted the relevant source of H_2O_2 in each type in Table 4 in the revised manuscript. Because organic peroxides are unstable and can easily decompose, off-line measurement of the aerosol-phase H_2O_2 could only obtain a snapshot of the decomposition process. Although there may be uncertainties regarding the aerosol-phase H_2O_2 measurement and the calculation of gas-aerosol partitioning coefficient of H_2O_2 , this paper provides new insights into understanding the gas-aerosol partitioning of H_2O_2 , as well as the sources and sinks of aerosol-phase H_2O_2 , which may contribute to the future studies related.

Provided that the influence of Teflon filters on the reactions of aerosol particles is so little as to be unnoticeable, the decomposition/hydrolysis rates of organic peroxides in aerosol particles on the filters are same as that in the atmosphere. It is well known that the decomposition/hydrolysis rates of organic peroxides are often positively related to the levels of organic peroxides. Due to the low aerosol water content of particles, the concentrations of aerosol-phase organic peroxides were ~ 5 orders of magnitude

higher than that in the extracted solution, which were estimated based on a comparison between the amount of the extracted solution and aerosol water content. The actual decomposition/hydrolysis rates in aerosol particles may be higher than that in the extracted solution. However, we cannot know how much the difference between them due to the limitations of the available measurement technique. Based on above analysis, to a large extent, the effective gas-aerosol partitioning coefficient estimated in this paper can represent the actual gas-aerosol partitioning of H_2O_2 .

Furthermore, it took around 40 min to extract and transport the sample to the observation site for H_2O_2 measurement. Organic peroxides in the extracted solution may decompose into H_2O_2 during the process, leading to overestimation of the effective gas-aerosol partitioning coefficient of H_2O_2 . Provided that the maximum decomposition/hydrolysis rate of organic peroxides was $0.10 \text{ ng } \mu\text{g}^{-1} \text{ h}^{-1}$ (line 355 in the revised manuscript), the corrected gas-aerosol partitioning coefficient averaged $6.9 \times 10^{-4} \text{ m}^3 \mu\text{g}^{-1}$, which was the lowest value due to the assumed maximum value of the decomposition/hydrolysis rate of organic peroxides. Because the corrected value of the effective gas-aerosol partitioning coefficient was still much higher than K_p^t , we did not correct the data. The above analysis has been added in the Supplement (lines 158–168).

In addition, the level of gas-phase H_2O_2 during BJ-2018 Winter was very low, only tens of pptv. Lengthening sampling time will increase the aerosol-phase H_2O_2 concentration and ensure accurate quantitative detection of H_2O_2 , but it will also introduce some unknown errors. Therefore, we will comprehensively consider to determine an optimal sampling time in the future study of the gas-aerosol partitioning of H_2O_2 .

Minor comments:

Q3. Literature-reported Henry's law constants of H_2O_2 varies across a certain range. The authors should justify why they used $8.4 \times 10^4 \text{ M/atm}$. Is this the recommended value by the JPL publication?

A3: Thanks for your suggestion. Henry's law constant of H_2O_2 ($8.4 \times 10^4 \text{ M atm}^{-1}$) used in this paper was quoted from Sander et al. (2011), which was published in JPL Publication 10-6. In addition, Sander (2015) sorted Henry's law constants of H_2O_2 based on the data reliability, and $8.4 \times 10^4 \text{ M atm}^{-1}$ ranked higher. In addition, the latest recommended value was $8.7 \times 10^4 \text{ M atm}^{-1}$ at 298 K (Burkholder et al., 2015), which was close to $8.4 \times 10^4 \text{ M atm}^{-1}$ used in this paper.

Q4. Line 139 – Is the $\text{PM}_{2.5}$ concentration a good indicator for C_{om} in a polluted environment like Beijing?

A4: Thanks for your suggestion. In previous studies, they used TSP in calculating the field-derived gas-aerosol partitioning coefficient and assumed that the weight fraction of the organic matter phase in TSP was 1 (Pankow et al., 1994; Odum et al., 1996; Shen et al., 2018; Qian et al., 2019). We have replaced " C_{om} " with "TSP" in Eq. (4) in the revised manuscript, and used the $\text{PM}_{2.5}$ mass concentration since TSP concentration was not available.

Q5. Line 150 – The authors state that when H_A^m was less than H_A^t , the samples followed Henry's law. Why? Shouldn't they agree (neither higher nor lower)?

A5: Thanks for your suggestion. The previous expression was inappropriate and we have redefined

whether rain samples followed Henry's law in the revised manuscript.

C5: Lines 168–171 in Sec. 3.1.1:

“We divided 52 rain samples into three types based on the comparison of the measured and predicted levels of H_2O_2 . When the difference between levels of the measured and predicted liquid-phase H_2O_2 fell within $\pm 20\%$, we suggested that these samples (Type B) followed Henry's law, and the remaining samples (Type A and C) did not agree with Henry's law. The percentages of samples in Type A, B and C were 69 %, 19 %, and 12 %, respectively.”

Q6. Line 275 – The authors report here that heterogeneous uptake can count for 86% of aerosol phase H_2O_2 . Later in Line 346, the author report 0.5%. Please clarify.

A6: Thanks for your suggestion. The two percentages are calculated in different methods. 86 % refers to the ratio of the amount of heterogeneous uptake of H_2O_2 to the measured aerosol-phase H_2O_2 level, while 0.5 % refers to the ratio of the amount of heterogeneous uptake of H_2O_2 to the consumption amount of aerosol-phase H_2O_2 . In addition, we have reevaluated the contribution of the heterogeneous uptake to the aerosol-phase H_2O_2 based on the formation and consumption rates according to the reviewers' suggestions, and the heterogeneous uptake could account for 2 % of the consumption rate of the aerosol-phase H_2O_2 . To avoid confusion, we have removed 86 % in Sec. 3.2.3 and 0.5 % in Sec. 3.3.

Q7. Line 370 – correct me if I am wrong. “additional source of liquid-phase H_2O_2 gradually increased” – should this be the sink of H_2O_2 due to droplet-to-gas transfer is gradually reduced?

A7: Yes, you are right. We have rewritten the description in the revised manuscript.

C7: Lines 450–451 in Sec. 4:

“In addition, the sink of H_2O_2 due to droplet-to-gas transfer was reduced with an increase in raindrop diameter, thus the liquid-phase H_2O_2 level also increased.”

Q8. Figure 5, and Line 263 – the authors interpret the inversely related H_2O_2 concentration and $\text{PM}_{2.5}$ /sulfate concentrations as results of a H_2O_2 sink by SO_2 oxidation. However, could the inversed relation be just due to dilution of H_2O_2 when aerosol loading is high?

A8: Thanks for your suggestion. We did not consider the dilution of H_2O_2 due to an increase in aerosol loading, and we have added it in the revised manuscript. To avoid the effects of outliers, we chose 10th and 90th percentiles of the levels of aerosol-phase H_2O_2 , SO_4^{2-} and $\text{PM}_{2.5}$ to explain the inverse relationship between H_2O_2 and $\text{SO}_4^{2-}/\text{PM}_{2.5}$. The extent of the concentration variations of H_2O_2 , SO_4^{2-} and $\text{PM}_{2.5}$ were 22, 6 and 5, respectively. Because the level of H_2O_2 changed more than that of SO_4^{2-} and $\text{PM}_{2.5}$, the inverse relationship still existed when we eliminated the interference of the dilution effect due to the high aerosol loading. In addition, the ratios of the extent of the concentration variations between H_2O_2 and $\text{SO}_4^{2-}/\text{PM}_{2.5}$ were equal to 4, indicating that a H_2O_2 sink by SO_2 oxidation was more important than the dilution effect and the dilution effect could be neglected.

C8: Lines 303–306 in Sec. 3.2.2:

“The extent of the concentration variations of H_2O_2 , SO_4^{2-} and $\text{PM}_{2.5}$ at 10th and 90th percentiles were 22, 6 and 5, respectively, suggesting that the inverse relationship still existed when we eliminated the

interference of the dilution effect due to a high aerosol loading. The dilution effect was unimportant and could be neglected.”

Technical comments:

Q9. Line 59 – “easily to absorbed” to “easily absorbed”.

A9: Yes, we have revised it in line 65.

Q10. Line 144 – “statistically counted” appears awkward. Should probably remove.

A10: Yes, we have removed it in line 160.

Q11. Line 146 – “with” 25.20 μM – is 25.20 μM the theoretical value? “with” makes the sentence unclear.

A11: Yes, we have replaced “with” with “is” in line 162.

Q12. Line 171 – “almost” less than 2000 m – should this be “always” less than 2000 m?

A12: Yes, we have changed “almost” into “always” in line 194.

References

- Burkholder, J. B., Sander, S. P., Abbatt, J. P. D., Barker, J. R., Huie, R. E., Kolb, C. E., Kurylo, M. J., Orkin, V. L., Wilmouth, D. M., and Wine, P. H.: Chemical kinetics and photochemical data for use in atmospheric studies, Evaluation No. 18, JPL Publication 15-10, Jet Propulsion Laboratory, Pasadena, <http://jpldataeval.jpl.nasa.gov> (last access: 19 March 2020), 2015.
- Odum, J. R., Hoffmann, T., Bowman, F., Collins, D., Flagan, R. C., and Seinfeld, J. H.: Gas/particle partitioning and secondary organic aerosol yields, *Environ. Sci. Technol.*, 30, 2580–2585, <https://doi.org/10.1021/es950943+>, 1996.
- Pankow, J. F.: An absorption model of gas-particle partitioning of organic compounds in the atmosphere, *Atmos. Environ.*, 28, 185–188, [https://doi.org/10.1016/1352-2310\(94\)90093-0](https://doi.org/10.1016/1352-2310(94)90093-0), 1994.
- Qian, X., Shen, H. Q., and Chen, Z. M.: Characterizing summer and winter carbonyl compounds in Beijing atmosphere, *Atmos. Environ.*, 214, 116845, <https://doi.org/10.1016/j.atmosenv.2019.116845>, 2019.
- Sander, R.: Compilation of Henry’s law constants (version 4.0) for water as solvent, *Atmos. Chem. Phys.*, 15, 4399–4981, <https://doi.org/10.5194/acp-15-4399-2015>, 2015.
- Sander, S. P., Abbatt, J., Barker, J. R., Burkholder, J. B., Friedl, R. R., Golden, D. M., Huie, R. E., Kolb, C. E., Kurylo, M. J., Moortgat, G. K., Orkin, V. L., and Wine, P. H.: Chemical kinetics and photochemical data for use in atmospheric studies, Evaluation No. 17, JPL Publication 10-6, Jet Propulsion Laboratory, Pasadena, <http://jpldataeval.jpl.nasa.gov> (last access: 19 March 2020), 2011.
- Shen, H. Q., Chen, Z. M., Li, H., Qian, X., Qin, X., and Shi, W. X.: Gas-particle partitioning of carbonyl compounds in the ambient atmosphere, *Environ. Sci. Technol.*, 52, 10997–11006, <https://doi.org/10.1021/acs.est.8b01882>, 2018.

Table 4: Comparison of the H₂O₂ evolution parameters in the extracted solution among the three types.

Parameters	First type	Second type	Third type
Peak time (h)	5	40	–
Decomposition rate of organic peroxides to H ₂ O ₂ (ng μg ⁻¹ h ⁻¹)	0.01	0.10	–
C_{max}/C_0 of H ₂ O ₂ (μM/μM)	1.52	39.22	1.00
TPOs/H ₂ O ₂ (μM/μM)	5.25	40.06	47.59
Ratio of decomposable organic peroxides (%)	29	98	0

Partitioning of hydrogen peroxide in gas-liquid and gas-aerosol phases

Xiaoning Xuan[†], Zhongming Chen[†], Yiwei Gong[†], Hengqing Shen[†], and Shiyi Chen[†]

[†]State Key Laboratory of Environmental Simulation and Pollution Control, College of Environmental Sciences and Engineering, Peking University, Beijing, 100871, China

Correspondence to: Zhongming Chen (zmchen@pku.edu.cn)

Abstract. Hydrogen peroxide (H_2O_2) is a vital oxidant in the atmosphere and plays critical roles in the oxidation chemistry of both liquid and aerosol phases. The partitioning of H_2O_2 between the gas and liquid phase or the aerosol phase could affect its abundance in these condensed phases and eventually the formation of secondary components. However, the partitioning processes of H_2O_2 in gas-liquid and gas-aerosol phases are still unclear, especially in the ambient atmosphere. In this study, field observations of gas-, liquid-, and aerosol-phase H_2O_2 were carried out in the urban atmosphere of Beijing during the summer and winter of 2018. The effective field-derived mean value of Henry's law constant (H_A^m , $2.1 \times 10^5 \text{ M atm}^{-1}$) was 2.5 times ~~that~~ of the theoretical value in pure water (H_A^t , $8.4 \times 10^4 \text{ M atm}^{-1}$) at $298 \pm 2 \text{ K}$. The effective derived gas-aerosol partitioning coefficient (K_P^m , $3.8 \times 10^{-3} \text{ m}^3 \mu\text{g}^{-1}$) was four orders of magnitude higher on average than the theoretical value (K_P^t , $2.8 \times 10^{-7} \text{ m}^3 \mu\text{g}^{-1}$) at $270 \pm 4 \text{ K}$. Beyond following Henry's law or Pankow's absorptive partitioning theory, The the partitioning of H_2O_2 in the gas-liquid and gas-aerosol phases in the ambient atmosphere ~~does not only obey Henry's law or Pankow's absorptive partitioning theory but~~ was also influenced by certain physical and chemical reactions. The average concentration of liquid-phase H_2O_2 in rainwater during summer was $44.12 \pm 26.49 \mu\text{M}$. In ~~three quarters~~ 69 % of the collected rain samples, the measured level of H_2O_2 was greater than the predicted value in pure water calculated by Henry's law. In these samples, ~~46-41 %~~ 46-41 % of the measured H_2O_2 was from gas-phase partitioning, ~~and while~~ most of the rest may ~~have come be~~ from residual H_2O_2 in raindrops. In winter, the level of aerosol-phase H_2O_2 was $0.093 \pm 0.085 \text{ ng } \mu\text{g}^{-1}$, which was much higher than the predicted value based on Pankow's absorptive partitioning theory. The contribution of partitioning of the gas-phase H_2O_2 to the aerosol-phase H_2O_2 formation was negligible. Almost all aerosol-phase H_2O_2 was not from the partitioning of the gas phase. The decomposition/hydrolysis rate of aerosol-phase organic peroxides could ~~be responsible~~ account for ~~11-74~~ 32 % of ~~the consumption rate of~~ aerosol-phase H_2O_2 , ~~and the value depended on the composition of organic peroxides in the aerosol particles. formation at the maximum rate of $3.65 \text{ ng } \mu\text{g}^{-1}$.~~ Furthermore, the heterogeneous uptake of HO_2 and H_2O_2 on aerosols contributed to 22 % and less than 2-0.5 % of the aerosol-phase H_2O_2 consumption, respectively.

1 Introduction

Hydrogen peroxide (H_2O_2) is a crucial oxidant in the liquid- and aerosol-phase chemistry, regarded as a significant oxidant in

the liquid and aerosol phases, is of great significance to the oxidation capacity in these phases (Reeves and Penkett, 2003). In addition to its direct effect as an oxidant, H_2O_2 also ~~Additionally, it~~ serves as ~~a~~the temporary reservoir species that cycles and redistributes the HO_x radicals (Lee et al., 2000; Tong et al., 2016; Crowley et al., 2018). Owing to ~~larger-high~~ solubility in water (O'Sullivan et al., 1996) and ~~larger-high~~ reaction rate with reduced substances (Seinfeld and Pandis, 2006), H_2O_2 plays a vital part in the fast formation of sulfate (SO_4^{2-}) and fine particles ($\text{PM}_{2.5}$) during heavy haze episodes (Stein and Saylor, 2012; Qin et al., 2018; Ye et al., 2018; Liu et al., 2020). ~~Furthermore~~Moreover, H_2O_2 as a typical reactive oxygen species (ROS), has adverse health effects and contributes to incidences of lung cancer, asthma, and cardiopulmonary disease (Gurgueira et al., 2002; Zhao et al., 2011; Campbell et al., 2019).

~~As is well known,~~ H_2O_2 in the liquid and aerosol phases is generally assumed to originate from the partitioning of gas-phase H_2O_2 . ~~Furthermore, and~~ the partitioning of H_2O_2 between the gas-liquid and gas-aerosol phases is expected to obey Henry's law and Pankow's absorptive partitioning theory, respectively. ~~Studies of Research on~~ the partitioning process of H_2O_2 ~~may~~ contribute to a clearer understanding of the sources of limiting oxidants, ~~as well as and estimates of~~ the contribution ~~of H_2O_2~~ to sulfate formation in the liquid and aerosol phases. In this study, we define the field-derived ratios of the measured levels of gas-to-liquid and gas-to-aerosol phases as the effective Henry's law constant and the ~~effective~~ gas-aerosol partitioning coefficient, respectively.

However, it is ~~noteworthy~~interesting that the predicted liquid-phase concentration of H_2O_2 in rainwater using Henry's law was not ~~sufficientenough~~ to account for the measured level, and a large amount of liquid-phase H_2O_2 was produced from other reactions (Liang et al., 2013). Chung et al. (2005) demonstrated that the "salting-in" effect could ~~as much as~~ double the solubility of H_2O_2 in salt solutions ~~with concentrations up to 10 M, but,~~ ~~However,~~ the ionic strength in rainwater ~~is was~~ too low to impose the "salting-in" effect (Li et al., 2019). Therefore, we need to seek other ~~possible~~ explanations. In addition, the ~~level of~~ gas-phase H_2O_2 ~~level~~ at the ground after a shower was higher than before, ~~revealing-suggesting~~ that raindrops could release H_2O_2 into the gas phase at the ground (Hua et al., 2008). This ~~opens-upprovided~~ new possibilities for explaining the high level of H_2O_2 in rainwater. ~~Nevertheless~~However, the falling of raindrops is a complex process that involves several uncertainties, so observational studies are needed to quantitatively explain the high concentration ~~of H_2O_2~~ in rainwater. The measured level of H_2O_2 in aerosol particles ~~was could be two orders of magnitude much~~ higher than the theoretical value ~~for from~~ gas-aerosol partitioning, ~~by two orders of magnitude~~ (Hasson and Paulson, 2003; Arellanes et al. 2006). ~~In previous studies,~~ and it was confirmed that considerable H_2O_2 could be produced from redox reactions in aerosols, ~~like (e.g.,~~ transition metals ~~involved)~~ (Charrier et al., 2014). However, it is noticeable that continuous redox reactions are assisted by available reductants, so it is impossible for ambient aerosols to generate H_2O_2 from transition metals ~~involved reactions~~ without an additional reduced agent (Shen et al., 2011). Recently, numerous studies have reported the decomposition of organic peroxides in the aerosol phase (Krapf et al., 2016; Riva et al., 2017). Li et al. (2016) suggested that the decomposition/hydrolysis of organic peroxides on secondary organic aerosol particles could substantially raise the level of H_2O_2 . Qiu et al. (2019) proposed that α -hydroxyalkyl-hydroperoxides could be easily decomposed into H_2O_2 within 2 h in $\geq 10\%$ water mixtures. However, the ~~quantitative measurement~~quantification of organic peroxides is difficult because of their instability (Zhao et al., 2018). The

decomposition of labile organic peroxides should be studied in ~~atmospheric~~ fine particles (~~PM_{2.5}~~) in heavily polluted areas. In addition, ~~as~~ H₂O₂ ~~is~~ easily ~~to~~ adsorbed and absorbed onto aerosol particles ([Zhao et al., 2011](#); [Wu et al., 2015](#)), its heterogeneous uptake should also be considered. Hence, ~~field measurements are needed for~~ a quantitative evaluation of ~~the sources of aerosol-phase H₂O₂~~, other than gas-phase partitioning ~~is needed with the support of field measurements~~.

Compared to gas-phase H₂O₂, it is challenging to quantitatively understand the chemistry of H₂O₂ in the liquid and aerosol phases. To the best of our knowledge, this is the first study to measure H₂O₂ in gas-liquid or gas-aerosol phases simultaneously in a heavily polluted area, ~~e.g., that is~~, Beijing, ~~which provided~~ a good opportunity to better understand the partitioning of H₂O₂ in different phases. The objectives of this study are to explore the partitioning of H₂O₂ in the gas-liquid and gas-aerosol phases in the ambient atmosphere, and to seek possible sources ~~other than in addition to~~ gas-phase partitioning that could increase H₂O₂ concentration in the liquid and aerosol phases.

2 Experimental

2.1 Measurement site

The online gas-phase measurement of peroxides was performed at the Peking University (PKU) site (39.99° N 116.30° E), situated in the northwest of urban Beijing. The PKU site is a typical city site in a heavily polluted area in Beijing, with two main trunks of traffic to the east and south. The relative apparatuses were placed on the roof of a building that was ~ 26 m above ground level. In this study, we introduced two measurements at the PKU site: BJ-2018Summer (23 July–10 August 2018 and 25 August–11 September 2018) and BJ-2018Winter (21 December 2018–5 January 2019).

2.2 Measurement methods

2.2.1 Gas-phase peroxides

The concentrations of gas-phase peroxides were ~~observed-measured~~ in both BJ-2018Summer and BJ-2018Winter using high performance liquid chromatography (HPLC, Agilent 1200, USA) with a time resolution of 21 min. The HPLC coupled with the post-column enzyme derivatization method could distinguish H₂O₂ from organic peroxides. This method is well established ([Hua et al., 2008](#); [He et al., 2010](#); [Wang et al., 2016](#)) and is only briefly described here. Ambient air was drawn into a glassy scrubbing coil at a flow rate of 2.7 standard L min⁻¹. H₃PO₄ solution (5 × 10⁻³ M) was added to the scrubbing coil at 0.2 mL min⁻¹ to dissolve H₂O₂ from ambient air. The collection efficiency of H₂O₂ was validated to ~~be~~ close to 100 %, ~~while it was 85 % for organic peroxides~~. Then, the mixture was injected into HPLC with the mobile phase (H₃PO₄, 5 × 10⁻³ M). Peroxides separated by the column reacted stoichiometrically with para-hydroxyphenylacetic acid (PHPAA) under the Hemin catalyst, generating stable PHPAA dimers that were measured by a fluorescence detector. The peroxides were identified and quantified using standard samples, and the detection limit (DL) of the gas-phase H₂O₂ was about 10 ~~parts per trillion by volume (pptv)~~. The values below DL were replaced by DL divided by the square root of two (the same hereafter). The gas-phase samples

during BJ-2018Summer were used for the partitioning analysis in the gas-liquid phase, while the data of BJ-2018Winter were used to study the partitioning in the gas-aerosol phase.

2.2.2 Liquid-phase peroxides

Rain samples were collected by a custom-built glass funnel and were used for the analysis of liquid-phase peroxides in BJ-2018Summer. During the observation period, the collection of rain samples was well organized depending on the intensity, amount, and duration of the rain. Because the peroxides were easy to break down, the collected rain samples were preserved in brown vials at 4°C/277 K until ~~they could be being~~ analysed with HPLC within 6 h. The subsequent detection method for the liquid-phase peroxides was the same as for the gas-phase peroxides. In all, we collected 60 rain samples during seven rain episodes, and the DL of the liquid-phase H₂O₂ was about 8 nM. The specific dates of the rain events in chronological order were 24 July, 25 July, 5 August, 6 August, 8 August, 30 August and 2 September.

2.2.3 Aerosol-phase peroxides

Aerosol-phase samples were gathered on Teflon filters (Whatman™, 47 mm diameter and 2 μm pore size) using a four-channel filter sampler (Wuhan Tianhong TH-16A, China) at 16.7 standard L min⁻¹ during BJ-2018Winter. Teflon filters were supported by stainless steel filter holders during ~~the a~~ 11.5 h sampling ~~time interval~~. We immediately disposed of two Teflon filters for the analysis of peroxides and total peroxides (TPOs), and the ~~remaining remained~~ filters were kept under refrigeration at ~~-18 °C/255 K~~ for subsequent component analysis. For analysing the aerosol-phase peroxides, the Teflon filters were immediately extracted with 10 mL H₃PO₄ in conical flasks and placed on a shaker to be blended thoroughly at 4°C/277 K and 180 rpm for 15 min. Then, the extracted solution was measured with HPLC within 40 min. The remained extracted solution was stored at 255 K away from light for subsequent measurement of H₂O₂ concentration variation with time, and details of the experimental conditions of the extracted solution are shown in the Supplement. Photochemical reactions of aerosols may produce aerosol-phase H₂O₂ (Zhou et al., 2008), and the effect of the photochemical reactions on the level of H₂O₂ in the extracted solution is discussed in the Supplement. Furthermore, ~~The the~~ extracted solution was also used for the measurement of TPOs using the iodometric spectrophotometric method, which could measure H₂O₂ as well as organic peroxides. (Nozaki, 1946; Banerjee and Budke, 1964). The extraction efficiency has been discussed in our previous work (Li et al., 2016) and we did not correct the total peroxides level. After the oxygen in the extracted solution was blown off by bubbling with nitrogen for 5 min, 250 μL potassium iodide solution (KI, 0.75 M) was added to the solution to react with TPOs in the dark for 12–24 h (Reactions R1 and R2). The reaction product I₃⁻ ion could be detected using UV/Vis spectrophotometry (Beijing PERSEE TU-1810, China) at the wavelength of 420 nm. A total of 31 aerosol-phase samples were analysed, and the DL of aerosol-phase H₂O₂ was close to 0.24 ng m⁻³ (0.006 ng μg⁻¹).

To avoid the matrix influence on samples (i.e., Teflon filters and the H₃PO₄ solution), we measured the concentration of blank samples in every extraction. The level of H₂O₂ in three-quarters of the blank samples was equal to 0 μM, and the concentration

of H₂O₂ in the remnant blank samples was below 10 % of that in the ambient ~~air~~aerosol samples. To prevent the matrix influence, we deducted the background values of the samples. In addition, to ensure that the measured H₂O₂ was attributed to aerosols collected on Teflon filters, we performed experiments to demonstrate that the physical adsorption on clean Teflon filters without aerosols was responsible for 15 % of the measured H₂O₂ in aerosol samples. The details are available in Fig. S1 in the Supplement. In this study, we did not correct the effect of the physical adsorption ~~to avoid introducing new errors~~ on the aerosol-phase H₂O₂.



2.2.4 Other components and meteorological parameters

Water-soluble cations (Na⁺, NH₄⁺, K⁺, Mg²⁺, and Ca²⁺) as well as anions (Cl⁻, NO₃⁻, and SO₄²⁻) were measured with ion chromatography (IC, Dionex ICS2000 and ICS2500, USA). Transition metal elements deposited on Teflon filters were measured with inductively coupled plasma mass spectrometry (ICP-MS, Bruker aurora M90, Germany). The mass concentration of PM_{2.5} was measured with a TEOM 1400a analyser. Meteorological parameters (ambient temperature, relative humidity, and wind speed) and major trace gases (O₃, SO₂, NO-NO₂-NO_x and CO) were monitored simultaneously using a series of commercial instruments (Met One Instruments Inc., Thermo 49i, 43i, 42i, and 48i).

2.3 Estimation of effective partitioning coefficients

To estimate the effective partitioning coefficients, we could use the field-derived Henry's law constant for the gas-liquid phase and the gas-aerosol partitioning coefficient for the gas-aerosol phase (Pankow, 1994), which are estimated according to Eqs.

(1) ~~to~~-(4):

$$H_A^t = 8.4 \times 10^4 \text{ M atm}^{-1} \quad (1)$$

$$H_A^m = \frac{C_{aq}^m}{C_g^m} \quad (2)$$

$$K_P^t = \frac{RT_W f_{om}}{10^6 \overline{MW}_{OM} \zeta p_L^0} \quad (3)$$

$$K_P^m = \frac{C_p^m}{C_g^m TSP C_{om}} \quad (4)$$

$$H_P^m = \frac{C_p^m}{C_g^m} \quad (5)$$

In Eqs. (1) and (2), C_{aq}^m is the liquid-phase level of H₂O₂, M; C_g^m is the partial pressure of the gas-phase H₂O₂, atm; and H_A^t and H_A^m are the theoretical values in pure water and the effective field-derived Henry's law constant, respectively, M atm⁻¹ (Sander et al., 2011). The average temperature during rainfall in summer (T_S) is 298 ± 2 K (mean ± standard deviation, the

145 same hereafter). In Eq. (3), K_p^t is the theoretical value of the gas-aerosol partitioning coefficient, $\text{m}^3 \mu\text{g}^{-1}$; \overline{MW}_{OM} is the
 estimated average molecular weight of organic compounds, 200 g mol^{-1} (Williams et al., 2010; Xie et al., 2014); p_L^0 is the
 vapour pressure of pure H_2O_2 at the specified temperature, calculated by the extrapolation of the Antoine equation (Maass and
 Hiebert, 1924; Baum et al., 1997); ζ is the activity coefficient of H_2O_2 , assumed to be unity (Pankow, 1994); f_{om} is the
 weight fraction of ~~the organic matter phase H_2O_2 in absorbing on aerosols~~TSP, also set to unity (~~Liang et al., 1997~~; Shen et al.,
 150 2018); R is the ideal gas constant, $8.2 \times 10^{-5} \text{ atm m}^3 \text{ mol}^{-1} \text{ K}^{-1}$; and T_w is the mean temperature during BJ-2018Winter, $270 \pm 4 \text{ K}$ for the whole observation period, $272 \pm 4 \text{ K}$ for day-time, and $269 \pm 4 \text{ K}$ for night-time. In Eq. (4), C_p^m and C_g^m are
 the concentrations of H_2O_2 in the aerosol and gas phases, respectively, $\mu\text{g m}^{-3}$; ~~C_{om}^{TSP} is the mass concentration of~~
~~suspended particles is the organic matter concentration, referring to the mass concentration of $\text{PM}_{2.5}$ is used here~~, $\mu\text{g m}^{-3}$; and
 K_p^m is the effective field-derived gas-aerosol partitioning coefficient, $\text{m}^3 \mu\text{g}^{-1}$. ~~In Eq. (5), H_p^m is the effective field-derived~~
 155 ~~Henry's law constant of H_2O_2 for the gas-aerosol phase, M atm^{-1} ; C_p^m (M) and C_g^m (atm) are aerosol- and gas-phase~~
~~concentrations of H_2O_2 .~~

3 Results and discussion

3.1 Gas-liquid phase partitioning

3.1.1 Gas- and liquid-phase H_2O_2 in summer

160 The concentration of gas-phase H_2O_2 was ~~statistically counted~~measured to be 0.30 ± 0.26 parts per billion by volume (ppbv)
 for the seven rainfalls (Fig. S2a in the Supplement) and 0.53 ± 0.77 ppbv for the entire BJ-2018Summer. ~~Compared with that~~
~~the theoretical liquid-phase H_2O_2 value in pure water with was 25.20 μM , and~~ the level of measured H_2O_2 in the liquid phase
 was $44.12 \pm 26.49 \mu\text{M}$ (3.19–139.95 μM), as shown in Fig. S2b. The detailed values of the peroxides in the gas and liquid
 phases are shown in Table S1. Based on Eq. (2), the effective field-derived Henry's law constant, H_A^m , averaged $2.1 \times 10^5 \text{ M}$
 165 atm^{-1} in rain samples, which was two and a half times the theoretical pure-water Henry's law constant, H_A^t , at $8.4 \times 10^4 \text{ M}$
 atm^{-1} and $298 \pm 2 \text{ K}$. ~~The average of the ratio of predicted to measured levels of H_2O_2 in each rain sample was 88 %.~~ The
~~analysis-result shows-suggested~~ that 88 % of the measured liquid-phase H_2O_2 came from gas-phase partitioning, while 12 %
 of H_2O_2 was from other sources. ~~We divided 52 rain samples into three types based on the comparison of the measured and~~
~~predicted levels of H_2O_2 . When the difference between levels of the measured and predicted liquid-phase H_2O_2 fell within \pm~~
 170 ~~20 %, we suggested that these samples (Type B) followed Henry's law, and the remaining samples (Type A and C) did not~~
~~agree with Henry's law. The percentages of samples in Type A, B and C were 69 %, 19 %, and 12 %, respectively. The details~~
~~of each rain sample are presented in Fig. 1. In this paper, we focused on the Type A samples with a high measured liquid-phase~~
 ~~H_2O_2 level, and the .In 23 % of the total rain samples, H_A^m was less than H_A^t , indicating that these samples followed Henry's~~
~~law (Fig. 1). In the remaining 77 69 % of the samples (i.e., Type A samples), the measured liquid phase H_2O_2 was larger higher~~
 175 ~~than the predicted values (Fig. 1), and the difference between levels of the measured and predicted liquid-phase H_2O_2 averaged~~

28–30 μM with a maximum of 71 μM . Further, based on the ratio of the predicted to measured levels of H_2O_2 in rainwater, 54
59 % of the liquid-phase H_2O_2 in these Type A samples was produced from other-sources other than gas-phase partitioning.
 To explain the difference between H_A^m and H_A^t , we should rule out the effects of pressure, pH, and T_S on H_A^t . First, to our
 knowledge, the influence of pressure on H_A^t can usually be neglected under conditions of less than 1 atm (Lind and Kok,
 1986). Also, H_A^t of H_2O_2 is independent of pH in the range of 4–7 (Xu et al., 2012); therefore, the present study does not
 consider the influences of pressure and pH on H_A^t . The temperature during BJ-2018Summer ~~can~~ could be divided into three
 ranges: 294–296 K, 297–299 K, and 300–306 K. The percentages of samples in these three temperature ranges were 25 %,
 63 %, and 12 %, respectively, and the ratios of H_A^m to H_A^t in the same temperature ranges were 1.4, 2.6, and 4.5, respectively.
 The maximum value of H_A^t in the range 294–306 K was $1.2 \times 10^5 \text{ M atm}^{-1}$, while H_A^m reached $4.2 \times 10^5 \text{ M atm}^{-1}$ at the 90th
 percentile. This suggests ~~eds~~ that the influence of T_S on H_A^m was negligible. The nonlinear relationship between H_A^m and T_S ,
 shown in Fig. S3, also indicated ~~ds~~ that T_S ~~plays-played~~ an unimportant role in determining H_A^m . Thus, other explanations were
~~needed to be explored to for~~ understanding the difference between H_A^m and H_A^t .

3.1.2 Process of raindrops falling

The solubility of H_2O_2 in clouds ~~was-is~~ larger-higher than that in the ground rainwater. There is a negative dependence of the
 solubility on temperature (Huang and Chen, 2010), which allows for the possibility of mass transfer of H_2O_2 from rainwater
 to the surrounding air when falling. Let us assume that the gas-phase H_2O_2 concentration is homogeneous and the rain droplet
 size remains constant during the ~~its~~ falling process. The diameter of the raindrops (D_p) is mainly distributed in the range of
 0.05–2.50 mm. Calculations were performed for typical droplet diameters at 0.1 mm, 0.5 mm, 1.0 mm and 2.0 mm. The height
 of the precipitation cloud base during summer time in north China was almost-always less than 2000 m (Shang et al., 2012)-
~~As a result, so~~ we assumed the fall distance to be 500 m, 1000 m, 1500 m, and 2000 m, respectively, which ~~are-remained the~~
 same to previous studies (Adamowicz, 1979; Levine and Schwartz, 1982). In the process of falling, it ~~is-was~~ necessary to
 consider the mass transfer resistance in the gas and liquid phases. However, it could be that the shear force generated on the
 raindrop surface when it fell improved the mixing rate in the droplet significantly; therefore, the liquid-phase mass transfer
 resistance was negligible (Pruppacher and Klett, 1997; Elperin and Fominykh, 2005). Thus, the overall mass transfer resistance
 reduced to the mass transfer resistance in the gas phase.

Here, we first discussed residual H_2O_2 in raindrops after a fall from a height of 1000 m. The temperature in clouds (T_S^c) was
 estimated to be 292 K, 6 K lower than the ground. H_A^t in pure water at 292 K was $1.4 \times 10^5 \text{ M atm}^{-1}$ (Sander et al., 2011).
 Provided that the droplet started at equilibrium with the cloud atmosphere and the level of H_2O_2 in the cloud atmosphere was
equal to the level near the ground ($0.30 \pm 0.26 \text{ ppbv}$), the initial level of liquid-phase H_2O_2 before falling (C_{aq}^0) was 42.87 μM .
 However, the equilibrium was broken when the raindrops fell as the ambient temperature increased. The mass transfer
 coefficient in the gas phase (k_g) can be calculated by Eqs. (S1) to ~~=(S4)~~ in the Supplement (Levine and Schwartz, 1982; Kumar,
 1985). The concentration of H_2O_2 in the droplet at the ground (C_{aq}^d) can be estimated by Eq. (S5). The results are presented in

Table 1, ~~which shows us demonstrating~~ that the large droplet has a small mass transfer coefficient. As a result, the liquid-phase H_2O_2 in the large raindrops ~~is was~~ more slowly released into the air. C_{aq}^d of the droplet diameter at 2.0 mm was close to C_{aq}^0 , while C_{aq}^d at 0.1 mm approximated the theoretical level of liquid-phase H_2O_2 in pure water at 298 K, as indicated by Fig. 2. The results ~~show demonstrated~~ that the effect of residual H_2O_2 in large raindrops on the level of H_2O_2 in ground rainwater levels could be of great importance.

Next, we investigated the influence of different fall distances on C_{aq}^d . The decreasing temperature at increasing fall distances caused larger H_A^t and C_{aq}^0 in clouds, and C_{aq}^d also increased. The wide gap of C_{aq}^d between different fall distances ~~is was~~ more visible for the large droplet, as seen in Fig. 2. Based on the above analysis, the residual H_2O_2 in large raindrops ~~can could~~ increase the H_2O_2 level in rainwater to a maximum of 48.81 μM at a fall distance of 2000 m, which could explain to a large extent the difference between the measured and predicted levels of H_2O_2 in rainwater.

Based on the rain intensity, seven rain events during BJ-2018-Summer could be divided into three types, as shown in Table S2 in the Supplement. Rain events in types I, II, and III have rain intensities $< 1 \text{ mm h}^{-1}$, $1\text{--}10 \text{ mm h}^{-1}$, and $> 10 \text{ mm h}^{-1}$, respectively. The larger the diameter of raindrops, the greater the rain intensity (Kumar, 1985). According to the above relationship between the diameter of raindrops and the level of liquid-phase H_2O_2 in the ground rainwater, the difference between the measured and predicted liquid-phase H_2O_2 levels should be greater as the hourly rain intensity increases. We found that the differences between C_{aq}^m and C_{aq}^t increased during the rain periods on 25 July and 5 August, during which the maximum hourly rain intensities were more than 10 mm h^{-1} . Because it is difficult for the liquid-phase H_2O_2 in heavy rains to diffuse into the gas phase, much H_2O_2 may be retained in the ground rainwater, which could well represent the level of H_2O_2 in cloud water.

During the rain episode on 1–2 September 2018, the concentration of gas-phase H_2O_2 decreased over time. However, there was a sudden rise from 0.47 ppbv at 1:03 local time (LT) to 0.66 ppbv at 1:46 LT, which subsequently dropped to 0.38 ppbv over time (Fig. 3a). Surprisingly, the difference between the measured and predicted levels of liquid-phase H_2O_2 reached a low value in the meantime, indicating that the increase in gas-phase H_2O_2 was due to the release of H_2O_2 from raindrops ~~that could that contained~~ high levels of H_2O_2 , as presented in Fig. 3b. Compared with Fig. S4 in the Supplement, which ~~describes described~~ the relationship between rain intensity and time, the rain intensity simultaneously dropped to 3.51 mm h^{-1} from 6.35 mm h^{-1} , consequently decreasing the diameter of the raindrops (Kumar, 1985) and increasing the mass transfer of H_2O_2 from rainwater to the gas phase. Provided that 20 μM H_2O_2 in rainwater was released into ambient air, the increase in the gas-phase H_2O_2 level was 0.24 ppbv, which was in accordance with the sudden rise during 1:03–1:46 LT on 1–2 September 2018.

The above analysis ~~is based on the assumption assumes~~ that the gas-phase H_2O_2 concentration is uniform. However, the distribution of gas-phase H_2O_2 at different heights may be complicated. We could use the average level of H_2O_2 in rainwater at the ground to estimate the concentrations of H_2O_2 in cloud water (C_{aq}^c) and the nearby atmosphere (C_g^c), as presented in Table 2. Assuming the simplest case, D_p is 1.0 mm, the fall distance is 1000 m, and the levels of H_2O_2 in the gas phase and rainwater at the ground are 0.30 ppbv and 44.12 μM at 298 K, respectively. Considering the release of H_2O_2 from raindrops into ambient

air during the falling process, the level of H₂O₂ in cloud water should be 47 μM. Based on Henry's law, the surrounding gas-phase H₂O₂ ~~may-should~~ be 0.33 ppbv, a little higher than that at the ground. When the fall distance is 500 m, 1500 m, and 2000 m, H₂O₂ in cloud water should be 46 μM, 49 μM, and 51 μM, respectively, and H₂O₂ in nearby ambient air could be 0.41 ppbv, 0.26 ppbv, and 0.21 ppbv, respectively.

3.2 Gas-aerosol phase partitioning

3.2.1 Gas- and aerosol-phase H₂O₂ in winter

From 21 December 2018 to 5 January 2019, the gas-phase H₂O₂ level was 24.08 ± 28.83 ~~parts-per-trillion-by-volume-(pptv)~~, as shown in Fig. S5a in the Supplement. We eluted Teflon filters with H₃PO₄ solution and measured the level of H₂O₂ in the extracted solution to calculate the aerosol-phase H₂O₂ concentration. The mass concentration of aerosol-phase H₂O₂ and the normalized concentration to aerosol mass were 2.22 ± 1.49 ng m⁻³ (~~<0.24DL~~-6.75 ng m⁻³) and 0.093 ± 0.085 ng μg⁻¹ (~~<0.006DL~~-0.409 ng μg⁻¹), respectively. The mean concentration of the aerosol-phase H₂O₂ at night-time (0.107 ± 0.102 ng μg⁻¹) was higher than that at day-time (0.079 ± 0.066 ng μg⁻¹), as presented in Fig. S5b. The level of aerosol-phase H₂O₂ in the present study was lower than those reported in previous studies (Table S3), which may be due to the extraction method, the extraction time, reduced substances levels, and aerosol pH values, as shown in the Supplement. Assuming a molecular weight of 300 g mol⁻¹ (Docherty et al., 2005; Epstein et al., 2014), the level of TPOs averaged 10.26 ± 6.38 ng μg⁻¹ (2.08–28.75 ng μg⁻¹). It was calculated that H₂O₂ took up a small fraction of TPOs, equal to 8 ± 6 % in molar concentration ratio, which indicated that organic peroxides accounted for a large proportion of peroxides, and could play important roles in the formation of PM_{2.5} and secondary organic aerosols.

The measured level of H₂O₂ in aerosols was much higher than the predicted value using Pankow's absorptive partitioning theory, which suggested that the aerosols collected on the filter existed under non-equilibrium conditions and the aerosol-phase H₂O₂ may arise from sources other than gas-phase partitioning ~~in the aerosol phase~~. Based on Eqs. (3) and (4), K_p^m was equal to $3.8 \times 10^{-3} \pm 4.8 \times 10^{-3}$ m³ μg⁻¹ at 270 ± 4 K, which was four orders of magnitude ~~more-higher~~ than K_p^t , 2.8×10^{-7} m³ μg⁻¹. The effect of parameter variation on calculating K_p^t (e.g., T_w , ζ , $\overline{MW_{OM}}$, and f_{om}) could not account for the large discrepancy between K_p^m and K_p^t (Shen et al., 2018), and other factors are needed to explain the difference. In terms of the proportion of theoretical to measured concentrations, the partitioning of gas-phase H₂O₂ into aerosols could be neglected, and nearly all of aerosol-phase H₂O₂ was generated from other reactions ~~besides gas phase partitioning~~.

Because aerosol water content (AWC) cannot be correctly evaluated at low RH, the effective field-derived Henry's law constant (H_p^m) of H₂O₂ was estimated for high RH condition, e.g. a heavy haze episode from 2 January to 3 January 2019 (RH, 30 %). Details regarding the estimation of AWC was shown in the Supplement. It was calculated that AWC, C_p^m and C_g^m levels averaged 3.20 μg m⁻³, 6.63×10^3 μM, and 1.90×10^{-11} atm. Based on Eq. (5), the average H_p^m on 2–3 January 2019 was calculated to be $2.7 \times 10^8 \pm 1.8 \times 10^8$ M atm⁻¹. However, the theoretical Henry's law constant (H_p^t) at 270 K was $1.1 \times$

275 10^6 M atm^{-1} (Sander et al., 2011), which was lower than H_p^m by two orders of magnitude. In Chung's study (2005), "salting-in" effect can improve the level of H_2O_2 by a factor of two when the concentrations in salt solutions were up to 10 M, and the most obvious "salting-in" effect of salt solutions was ammonium sulfate. In this paper, the levels of aerosol-phase NH_4^+ and SO_4^{2-} on 2–3 January 2019 were 94 M and 21 M, respectively, and the level of $(\text{NH}_4)_2\text{SO}_4$ was assumed to be 21 M. The increasement of H_p^m by the "salting-in" effect of $(\text{NH}_4)_2\text{SO}_4$ was about $3.2 \times 10^6 \text{ M atm}^{-1}$ at 286 K based on equations in Chung et al. (2005). Even though aerosol particles were collected at $270 \pm 4 \text{ K}$ and the increasement may be greater, the "salting-in" effect could not fully explain the difference between H_p^m and H_p^t . Other sources need to be found later.

280 ~~The level of aerosol-phase H_2O_2 in the present study was lower than those reported in previous studies (Table S3), which may be due to the extraction method, the extraction time, reduced substance levels, and aerosol pH values, as shown in the Supplement. Assuming a molecular weight of 300 g mol^{-1} (Decherty et al., 2005; Epstein et al., 2014), the level of TPOs averaged $10.26 \pm 6.38 \text{ ng } \mu\text{g}^{-1}$ ($2.08\text{--}28.75 \text{ ng } \mu\text{g}^{-1}$). It was calculated that H_2O_2 took up a small fraction of TPOs, equal to $8 \pm 6\%$ in molar concentration ratio, which indicated that organic peroxides accounted for a large proportion of peroxides, and could play important roles in the formation of $\text{PM}_{2.5}$ and secondary organic aerosols.~~

285 3.2.2 Factor analysis

Figure 4 ~~shows~~ demonstrated that the concentration of aerosol-phase H_2O_2 ~~is~~ was dependent on RH, with a trend of first increasing and then decreasing as RH ~~increases~~ increased. The variation of H_2O_2 with RH was the result of competition between production and consumption processes. Here, the production process refers to either process that favours increasing the level of aerosol-phase H_2O_2 , while the consumption process denotes ~~those~~ the processes consuming aerosol-phase H_2O_2 . In the first stage, the higher RH could accelerate the heterogeneous uptake of H_2O_2 onto aerosols and enhance the level of aerosol-phase H_2O_2 (Pradhan et al., 2010; Shiraiwa et al., 2011; Zhao et al., 2013; Slade and Knopf, 2015). The level of H_2O_2 ~~was~~ negatively associated with RH in the subsequent stage, ascribed to ~~the~~ much more rapid consumption of H_2O_2 due to its oxidizing the reduced substances on polluted days, such as SO_2 into SO_4^{2-} , ~~on polluted days~~.

295 We considered a heavy haze episode, from 2 January to 3 January 2019, as an example to explain ~~in detail~~ the important contribution of aerosol-phase H_2O_2 to SO_4^{2-} growth on polluted days in detail. The $\text{PM}_{2.5}$ mass concentration of the severe haze event was up to $201.20 \text{ } \mu\text{g m}^{-3}$. ~~The estimation of aerosol water content is shown in the Supplement.~~ Based on the measured H_2O_2 , the reaction rate (RR) and sulfate formation rate (SFR) averaged about $3.03 \times 10^{-3} \text{ } \mu\text{mol m}^{-3} \text{ h}^{-1}$ and $0.29 \text{ } \mu\text{g m}^{-3} \text{ h}^{-1}$ (Table S4), respectively. The detailed calculation process is provided in the Supplement. In addition, the growth rate of SO_4^{2-} calculated by the measured data was $0.51 \text{ } \mu\text{g m}^{-3} \text{ h}^{-1}$, and accounting for about 9 % of the observed formation of ~~$\text{PM}_{2.5}$~~ H_2O_2 oxidation pathway contributed about 57 % of the measured growth of SO_4^{2-} in $\text{PM}_{2.5}$. This result strongly suggested that the aerosol-phase H_2O_2 indeed acted as ~~the~~ an important oxidant in the formation of sulfate, and played significant roles in the rapid growth of $\text{PM}_{2.5}$ during pollution events.

300 Next, we considered that the consumption rate of aerosol-phase H_2O_2 increased with an increase of RH. The extent of the

concentration variations of H_2O_2 , SO_4^{2-} and $\text{PM}_{2.5}$ at 10th and 90th percentiles were 22, 6 and 5, respectively, suggesting that the inverse relationship still existed when we eliminated the interference of the dilution effect due to a high aerosol loading. The dilution effect was unimportant and could be neglected. It is suggested that larger levels of SO_4^{2-} and $\text{PM}_{2.5}$ are often accompanied by higher RH. In Fig. 5, the reverse curve between aerosol-phase SO_4^{2-} and H_2O_2 got became steeper with the formation of SO_4^{2-} , indicating that the rate of consumption of H_2O_2 on polluted days was much higher than that on clean days, which could offer proof of rapid H_2O_2 consumption with increasing RH. In addition, the level of H_2O_2 in the aerosol phase exhibited a negative correlation with $\text{PM}_{2.5}$ mass concentration, as shown in Fig. 5. In other words, the aerosol-phase H_2O_2 concentration was lower on polluted days than on clean days, which further demonstrates that the removal rate of H_2O_2 by oxidizing SO_2 into SO_4^{2-} exceeded the production rate during pollution events with high RH.

3.2.3 Heterogenous uptake of H_2O_2 and HO_2

In addition to the factors that influencing-influence the aerosol-phase H_2O_2 concentration, there are certain other physical and chemical reactions besides-other than gas-phase partitioning that could increase the level of aerosol-phase H_2O_2 , e.g., heterogeneous uptake of H_2O_2 on aerosols. Previous studies have shown that heterogeneous uptake of H_2O_2 is positively related with RH. High RH is beneficial to the mass transfer of H_2O_2 from the gas phase to the aerosol phase, which could accelerating the reaction between H_2O_2 and reduced compositions of aerosols, thus contributing to the more heterogenous uptake of H_2O_2 (Huang et al., 2015; Wu et al., 2015). To quantitatively evaluate the importance of the heterogeneous uptake of H_2O_2 on aerosols to the aerosol-phase H_2O_2 , we calculated the average rate of total heterogeneous uptake during the sampling process based on Eqs. (S6) to (S11) in the Supplement. Details about each parameter were introduced in Table 3, and. Compared with the averaged measured content of aerosol-phase H_2O_2 ($[\text{X}]_p^m$, $0.057 \text{ ng } \mu\text{g}^{-1}$), the total heterogeneous uptake rate of H_2O_2 ($d[\text{X}]_p^{t,h}/dt$) averaged $0.049\text{--}0.02 \text{ ng } \mu\text{g}^{-1} \text{ h}^{-1}$, indicating that heterogeneous uptake of H_2O_2 could account for 86 % of the measured level of H_2O_2 in the aerosol phase.

As HO_2 radical is a precursor of H_2O_2 , the heterogeneous uptake of HO_2 onto aerosols may also contribute to the formation of the aerosol-phase H_2O_2 . We assumed that the reactive uptake coefficient of HO_2 to aerosol particles was 0.2, and the product of HO_2 was H_2O_2 (Li et al., 2019). At the same observation site in winter of 2017, HO_2 concentration for noontime averaged $(0.4 \pm 0.2) \times 10^8 \text{ cm}^{-3}$ and $(0.3 \pm 0.2) \times 10^8 \text{ cm}^{-3}$ on clean and polluted days, respectively (Ma et al., 2019). Since HO_2 level data in 2018 was not available, we used the level of HO_2 on clean days in winter of 2017 for calculations, and the average was about $0.2 \times 10^8 \text{ cm}^{-3}$ at day-time. The heterogenous uptake rate of HO_2 on aerosols was calculated in the same way as H_2O_2 , and the formation rate of the aerosol-phase H_2O_2 by reactive uptake of HO_2 averaged $0.22 \text{ ng } \mu\text{g}^{-1} \text{ h}^{-1}$ at all day.

3.2.4 Decomposition of organic peroxides

It was found-demonstrated that the concentration of H_2O_2 in the extracted solution first increased rapidly, then reached peaks at distinct hours that depended on the particular-specific sample, and finally gradually declined gradually over time. However,

335 interestingly, there was large sample-to-sample variation, with samples classifiable into three types in terms of the change trend and evolution duration (Fig. 6 and Table 4). The third type (Fig. 6c) occurred when H₂O₂ level exhibited a steady decline from 0.03 μ M without a growth stage within 13 h, and this was the case with samples 5 and 6 on a slightly polluted day on 2 January 2019. Samples 1 and 2 on 29 December 2018 during clean days belonged to the first type (Fig. 6a), in which H₂O₂ rapidly grew within 5 h and subsequently decreased at a slow rate over 25 h. The evolution trends of H₂O₂ in the second type (samples 3 and 4, Fig. 6b) during clean days from 31 December 2018 to 1 January 2019 were similar to those of the first type, except H₂O₂ approached its peak at about 40 h over the whole analysis process lasting for about 300 h. Given that the H₂O₂ concentration increased in the extracted solution as time went, the effects of the extraction and transportation processes on the effective gas-aerosol partitioning coefficient of H₂O₂ were discussed, as shown in the Supplement.

340 To seek the reasons for the elevated level of H₂O₂ in the extracted solution, we compared the ratio of the maximum (C_{max}) to initial (C_0) H₂O₂ concentrations in the extracted solution with the molar concentration ratio of the aerosol-phase TPOs to H₂O₂ and found that the ratios of C_{max}/C_0 and TPOs/H₂O₂ were in the same order of magnitude for the first and second types, as exhibited in Table S5 in the Supplement. This result provided evidence that part of aerosol-phase H₂O₂ was originated from the decomposition/hydrolysis of organic peroxides, as described in earlier studies (Wang et al., 2011; Li et al., 2016). In the second type, the concentration of TPOs normalized to aerosol mass reached a maximum, indicating that the second type had more TPOs sources and which consequently caused higher TPOs/H₂O₂ and C_{max}/C_0 ratios compared with the first type. Furthermore, the aerosol surface is semi-liquid or liquid under high RH (Liu et al., 2017), which provides reaction sites for the decomposition/hydrolysis of aerosol-phase organic peroxides. Aerosol-phase organic peroxides could decompose into H₂O₂ before when the particle aerosols were being collected (Zhao et al., 2018). Thus, the decomposition/hydrolysis of organic peroxides in the extracted solution could be applied to the ambient particles. The average rates of the decomposition/hydrolysis of organic peroxides to H₂O₂ in the rising stage for the first and second types were 0.14–0.01 $\text{ng } \mu\text{g}^{-1} \text{ h}^{-1}$ and 3.65–0.10 $\text{ng } \mu\text{g}^{-1} \text{ h}^{-1}$, respectively.

350 The three types of samples were in accordance with the growth process of PM_{2.5}. According to meteorological parameters and trace gases data (Table S6 in the Supplement), static weather conditions gradually formed and were accompanied by lower wind speed, lower ozone level, higher RH, and higher gaseous pollutants levels. The mass concentration of PM_{2.5} increased from 13.45 $\mu\text{g m}^{-3}$ to 63.11 $\mu\text{g m}^{-3}$. In addition, the mass concentration of TPOs also showed a rising trend, however, whereas the level of TPOs normalized to aerosol mass increased at first and decreased afterwards due to the rapid growth of PM_{2.5}. Because of the consumption of reactive TPOs which formed SO₄²⁻ during polluted days, the rest of the TPOs were stable organic peroxides that could not easily decompose into H₂O₂, e.g., peroxide esters (ROOR). The ratio of TPOs/H₂O₂ in the third type, collected on a slightly polluted day, was close to that in the second type on clean days, but a rising trend of H₂O₂ in the extracted solution could not be observed. It was calculated that the ratios of decomposable TPOs to total TPOs for the three types were 29 %, 98 %, and 0 %, respectively.

365 Recently, it was reported that organic peroxides accounted for a large proportion of secondary organic aerosol (SOA) mass,

varying widely from less than 20 % to 60 % (Docherty et al., 2005; Li et al., 2016; Gong et al., 2018). Peroxy radicals also played important parts in the formation of highly oxygenated molecules (HOMs) via an autoxidation mechanism, which can form aerosols without sulfuric acid nucleation (Kirkby et al., 2016). The thermal decomposition of peroxide-containing SOAs and HOMs contributed to the formation of aerosol-phase H₂O₂ (Krapf et al., 2016). A similar phenomenon was also found by Li et al. (2016), in which the decomposition/hydrolysis of organic peroxides sustainably generated H₂O₂ accompanied by the attenuation of TPOs in the extracted solution, and about 18 % of gaseous organic peroxides experienced-underwent the heterogeneous decomposition on aerosols into H₂O₂. The decomposable organic peroxides are often peroxydicarboxylic acids (PCAs, e.g., peroxyacetic acid, PAA; peroxyformic acid, PFA) and α -hydroxyalkyl-hydroperoxides (α -HAHPs, e.g., hydroxymethyl hydroperoxide, HMHP). ~~Based on previous studies and the evolution trend of the three types in this study, we speculate that PCAs and α -HAHPs accounted for a large proportion of the first and second types, while ROOR played a large part in the third type, as shown in Table 4.~~

3.3 Source and sink of H₂O₂ in rainwater and aerosols

To provide support for the sources suggested above, we analysed the sources and sinks of liquid- and aerosol-phase H₂O₂ in rainwater and aerosols. In this study, the measured level of H₂O₂ was the concentration after partial or complete reaction with reduced substances, such as SO₂ onto the particles. The contribution of different additional sources in the liquid and aerosol phases should be estimated compared with the important sink.

The level of liquid-phase H₂O₂ level was the result of the combined effect between sources (gas-phase partitioning and residual H₂O₂ in raindrops) and sinks (reaction with S(IV) and the decomposition of H₂O₂). Based on the foregoing description, the dissolved gas-phase H₂O₂ in rainwater was 25.20 μ M at 298 K. The residual H₂O₂ in raindrops could enhance the level of liquid-phase H₂O₂ by up to 48.81 μ M, ~~based on Henry's law~~. The largest removal pathway of liquid-phase H₂O₂ was to the consumption by its oxidizing dissolved SO₂ into sulfate. Given that the major oxidants to sulfate formation were only H₂O₂ and O₃ (Penkett et al., 1979; Chandler et al., 1988), the proportions of the H₂O₂ oxidation pathway to the overall, calculated by Eqs. (S12) and (S13) in the Supplement, were 92 % at pH 5 and 11 % at pH 6, respectively. The average of sulfate concentration in rainwater was measured to be 31.95 μ M, and the H₂O₂ oxidation pathway contributed to the sulfate with 29 μ M at pH 5 and 4 μ M at pH 6, which was the consumption level-molar concentration of H₂O₂. In addition, the decomposition of H₂O₂ during 6 h storage time before analysis was 6 μ M (Li et al., 2016). To summarize, the concentration of liquid-phase H₂O₂ was supposed to have its maximum at 64.01 μ M, a bit lower than the 90th percentile of the measured level (67.85 μ M). This could be considered to achieve the approximate balance between sources and sinks in the liquid-phase H₂O₂. Consequently, the residual H₂O₂ in raindrops could explain the difference between H_A^m and H_A^t .

~~In terms of~~With respect to the sources and sinks for aerosol-phase H₂O₂, the main removal pathway was the consumption of H₂O₂ to sulfate formation, similar to the sink of H₂O₂ in the liquid phase. The average mass concentrations of PM_{2.5} and aerosol-phase SO₄²⁻ were 39.21 μ g m⁻³ and 2.20 μ g m⁻³, respectively. The mass concentration ratio of SO₄²⁻ to PM_{2.5} was 6 %

in this study, which was lower than previous studies (Ho et al., 2016; Shao et al., 2018). The discrepancy may be ~~accounted~~ explained by the decreased ratio of SO_4^{2-} to $\text{PM}_{2.5}$ due to SO_2 emissions control in recent years, as shown in the Supplement. Accordingly, the H_2O_2 -oxidation pathway accounted for 57 % of the sulfate formation in a typical haze event on 2–3 January 2019, and the consumption of aerosol phase H_2O_2 caused by sulfate formation maximized at $11.33 \text{ ng } \mu\text{g}^{-1}$. In this study, the maximum amount of H_2O_2 formed by the decomposition/hydrolysis of organic peroxides was close to $3.65 \text{ ng } \mu\text{g}^{-1}$, accounting for 32 % of the H_2O_2 formation in the aerosol phase. The heterogeneous uptake of H_2O_2 on aerosols had a minor contribution to the aerosol-phase H_2O_2 , and the proportion was less than 0.5 %. The sources could not achieve a balance with the consumption of the aerosol phase H_2O_2 . Provided that the γ value could reach 10^{-3} (Wang et al., 2016), the amount of heterogeneous uptake could reach $0.49 \text{ ng } \mu\text{g}^{-1}$. However, this still does not bridge the difference between sinks and sources. In our view, there are a couple of possible explanations for the difference. First, we estimated the contribution of the H_2O_2 oxidation pathway to sulfate formation during the entire measurement period based on the contribution of high pollution days, which may overestimate the sink for the aerosol phase H_2O_2 . Provided that the contribution ratio was 20 % on clean days, the sink for aerosol phase H_2O_2 to sulfate formation could be $3.97 \text{ ng } \mu\text{g}^{-1}$, which was in general accordance with the sources for aerosol phase H_2O_2 . Second, the inverse dependence of the γ value on the gas phase H_2O_2 concentration was not considered, and the γ value could have been underestimated when the level of gas phase H_2O_2 in winter was much lower (Romanias et al., 2012; Romanias et al., 2013). Third, there may be missing sources in aerosol phase H_2O_2 . There are possibly some potential sources that are not completely understood, such as the heterogeneous uptake of HO_2 on aerosols forming aerosol phase H_2O_2 (Liang et al., 2013) and so on. We estimated the contribution of different sources to the aerosol-phase H_2O_2 based on the formation and consumption rates. According to the previous estimation of the theoretical sulfate formation rate from January 2 to January 3 2019 ($0.29 \text{ } \mu\text{g m}^{-3} \text{ h}^{-1}$) and the average mass concentration of $\text{PM}_{2.5}$ ($106.19 \text{ } \mu\text{g m}^{-3}$), the consumption rate of H_2O_2 should be $0.97 \text{ ng } \mu\text{g}^{-1} \text{ h}^{-1}$. With respect to the sources of the aerosol-phase H_2O_2 , the decomposition/hydrolysis of organic peroxides was firstly considered, with average rates of the rising stage for the first and second types (Fig. 6), $0.01 \text{ ng } \mu\text{g}^{-1} \text{ h}^{-1}$ and $0.10 \text{ ng } \mu\text{g}^{-1} \text{ h}^{-1}$, respectively. Because the extracted solution was stored under 255 K, lower than the actual atmospheric temperature (270 K), the decomposition/hydrolysis rates of organic peroxides were underestimated and an adjusting factor should be multiplied. The factors for the three typical labile organic peroxides (HMHP, PFA, and PAA) were 13, 3, and 2, respectively, as shown in the Supplement. Assuming the factor was in the range of 2–13, the average decomposition/hydrolysis rate of organic peroxides for the first and second types ($0.055 \text{ ng } \mu\text{g}^{-1} \text{ h}^{-1}$) was used to calculate the formation rate. The formation rate of the aerosol-phase H_2O_2 from the decomposition/hydrolysis of organic peroxides could account for 11–74 % of the consumption rate by sulfate formation. Moreover, the heterogenous uptake of HO_2 and H_2O_2 were also likely to improve the aerosol-phase H_2O_2 level at the rates of $0.22 \text{ ng } \mu\text{g}^{-1} \text{ h}^{-1}$ and $0.02 \text{ ng } \mu\text{g}^{-1} \text{ h}^{-1}$, respectively, which can offset 22 % and 2 % of the consumption rate of H_2O_2 , respectively. The sources and sinks rates of H_2O_2 ~~do~~ did not seem to reach a balance. In our view, there ~~are~~ were a couple of possible explanations for the difference. First, we estimated the contribution of the H_2O_2 oxidation pathway to sulfate formation during the entire measurement period based on the contribution

of high-pollution days, which may overestimate the sink for the aerosol-phase H_2O_2 . Second, the inverse dependence of the γ value on the gas-phase H_2O_2 concentration was not considered, and the γ value could ~~have been be~~ underestimated when the level of gas-phase H_2O_2 in winter was much lower (Romanias et al., 2012; Romanias et al., 2013). Third, there may be missing sources in aerosol-phase H_2O_2 , which are not completely understood.

Based on the above analysis, sources and sinks of H_2O_2 in the liquid phase could achieve balance, while the formation of H_2O_2 from the decomposition/hydrolysis of aerosol-phase organic peroxides and the heterogeneous uptake of ~~HO_2 and~~ H_2O_2 could not offset the consumption of H_2O_2 in the aerosol phase. ~~Two-thirds of the total aerosol-phase H_2O_2 formation failed to be explained by the two possible sources.~~ Field measurements and laboratory experiments are urgently needed to further study the possible reasons and search for ~~other potential missing~~ sources of aerosol-phase H_2O_2 .

4 Conclusions

In this study, we simultaneously measured H_2O_2 concentrations in gas and rainwater in summer as well as in the gas and aerosol phases ($\text{PM}_{2.5}$) in winter over urban Beijing. For the investigated seven rain episodes, the average H_A^m was $2.1 \times 10^5 \text{ M atm}^{-1}$, which was 2.5 times greater than H_A^t at $298 \pm 2 \text{ K}$. The liquid-phase concentration of H_2O_2 averaged $44.12 \pm 26.49 \text{ }\mu\text{M}$. In ~~77~~ 69 % of the rain samples, the liquid-phase H_2O_2 level was much ~~larger~~ higher than the predicted values estimated for pure water using Henry's law. We found that 12 % of measured H_2O_2 in all samples and ~~54-59~~ % of measured H_2O_2 in those samples with high level of measured liquid-phase H_2O_2 level that did not follow Henry's law were from residual H_2O_2 in raindrops. With an increase in ~~raindrops diameter and~~ fall distance, the proportion of the additional source of liquid-phase H_2O_2 gradually increased. In addition, the sink of H_2O_2 due to droplet-to-gas transfer was reduced with an increase in raindrop diameter, thus the liquid-phase H_2O_2 level also increased. Furthermore, the source and sink of H_2O_2 in rainwater could achieve a balance.

For the measured $\text{PM}_{2.5}$ aerosol samples, a similar phenomenon was observed between the measured and predicted levels of H_2O_2 in the aerosol phase, but the difference was much higher than that in the liquid phase. K_p^m averaged $3.8 \times 10^{-3} \text{ m}^3 \mu\text{g}^{-1}$, which was four orders of magnitude higher than K_p^t at $270 \pm 4 \text{ K}$. The aerosol-phase concentration of H_2O_2 normalized to the aerosol mass averaged $0.093 \pm 0.085 \text{ ng }\mu\text{g}^{-1}$. ~~Aerosol-phase H_2O_2 level was associated with relative humidity, increasing before decreasing, which resulted from the competition between the formation and consumption of H_2O_2 .~~ The decomposition/hydrolysis of organic peroxides produced the elevated aerosol-phase H_2O_2 at a maximum rate of $0.10 \text{ ng }\mu\text{g}^{-1} \text{ h}^{-1}$, $3.65 \text{ ng }\mu\text{g}^{-1}$; which was responsible for ~~11-74 %~~ 32 % of the ~~consumption rate of formation of~~ aerosol-phase H_2O_2 , and its value depended on the composition of organic peroxides in the aerosol particles. The heterogeneous uptake of ~~HO_2 and~~ H_2O_2 played a minor role in increasing the H_2O_2 level in the aerosol phase, and the proportions based on the consumption rate of H_2O_2 was ~~were~~ 22 % and 2 % less than 0.5 %, respectively. There are many uncertainties in the decomposition/hydrolysis of organic peroxides in this study, and laboratory simulation studies are needed to quantify the roles of different organic peroxides in the decomposition process. Aerosol-phase H_2O_2 in this study cannot reach source and sink equilibrium, and there are missing sources of aerosol-phase H_2O_2 . Due to a lack of substantial severe haze events with high RH in this study, the

465 source and sink mentioned in the aerosol-phase H_2O_2 need to be further verified.
Our study has provided direct evidence to prove that the partitioning of H_2O_2 between the gas-liquid and gas-aerosol phases not only follows thermodynamic equilibrium but is affected by certain physical and chemical reactions. The effective field-derived Henry's law constant and gas-aerosol partitioning coefficient should be accepted to better predict the measured liquid- and aerosol-phase H_2O_2 concentrations, which would be beneficial to correctly calculating the contribution of H_2O_2 to the fast
470 formation of SO_4^{2-} and $\text{PM}_{2.5}$ during pollution episodes. More laboratory experiments and field measurements are urgently needed to improve our understanding of the partitioning of peroxides in different phases in the atmosphere.

Data availability. The data are accessible by contacting the corresponding author (zmchen@pku.edu.cn).

475 *Author contributions.* In the framework of BJ-2018Summer and BJ-2018Winter measurements, ZC and XX designed the study. XX carried out all peroxide measurements used in this study, analysed the data, and wrote the paper. ZC helped interpret the results, guided the writing, and modified the manuscript. YG contributed to the methods of analysing aerosol-phase hydrogen peroxides and total peroxides. HS helped interpret data and modified the paper. SC provided the data for the meteorological parameters, trace gases, and $\text{PM}_{2.5}$ mass concentrations. All authors discussed the results and contributed to the final paper.

480 *Competing interests.* The authors declare that they have no conflict of interest.

Acknowledgements. This work was funded by the National Key Research and Development Program of China (Grants 2016YFC0202704), National Research Program for Key Issues in Air Pollution Control (Grants DQGG0103) and the National
485 Natural Science Foundation of China (Grants 21477002).

References

- Adamowicz, R. F.: A model for the reversible washout of sulfur-dioxide, ammonia and carbon-dioxide from a polluted atmosphere and the production of sulfates in raindrops, *Atmos. Environ.*, 13, 105–121, [https://doi.org/10.1016/0004-6981\(79\)90250-6](https://doi.org/10.1016/0004-6981(79)90250-6), 1979.
- Arellanes, C., Paulson, S. E., Fine, P. M., and Sioutas, C.: Exceeding of Henry's law by hydrogen peroxide associated with urban aerosols, *Environ. Sci. Technol.*, 40, 4859–4866, <https://doi.org/10.1021/es0513786>, 2006.
- Banerjee, D. K. and Budke, C. C.: Spectrophotometric determination of traces of peroxides in organic solvents, *Anal. Chem.*, 36, 792–796, <https://doi.org/10.1021/ac60210a027>, 1964.
- Baum, E. J.: Chemical property estimation: theory and application, CRC Press Inc., Grand Valley State university, the United States of America, 1997.
- Campbell, S. J., Stevanovic, S., Miljevic, B., Bottle, S. E., Ristovski, Z., and Kalberer, M.: Quantification of particle-bound organic radicals in secondary organic aerosol, *Environ. Sci. Technol.*, 53, 6729–6737, <https://doi.org/10.1021/acs.est.9b00825>, 2019.
- Chandler, A. S., Choularton, T. W., Dollard, G. J., Eggleton, A. E. J., Gay, M. J., Hill, T. A., Jones, B. M. R., Tyler, B. J., Bandy, B. J., and Penkett, S. A.: Measurements of H₂O₂ and SO₂ in clouds and estimates of their reaction rate, *Nature*, 336, 562–565, <https://doi.org/10.1038/336562a0>, 1988.
- Charrier, J. G., McFall, A. S., Richards-Henderson, N. K., and Anastasio, C.: Hydrogen peroxide formation in a surrogate lung fluid by transition metals and quinones present in particulate matter, *Environ. Sci. Technol.*, 48, 7010–7017, <https://doi.org/10.1021/es501011w>, 2014.
- Chung, M. Y., Muthana, S., Paluyo, R. N., and Hasson, A. S.: Measurements of effective Henry's law constants for hydrogen peroxide in concentrated salt solutions, *Atmos. Environ.*, 39, 2981–2989, <https://doi.org/10.1016/j.atmosenv.2005.01.025>, 2005.
- Crowley, J. N., Pouvesle, N., Phillips, G. J., Axinte, R., Fischer, H., Petäjä, T., Nölscher, A., Williams, J., Hens, K., Harder, H., Martinez-Harder, M., Novelli, A., Kubistin, D., Bohn, B., and Lelieveld, J.: Insights into HO_x and RO_x chemistry in the boreal forest via measurement of peroxyacetic acid, peroxyacetic nitric anhydride (PAN) and hydrogen peroxide, *Atmos. Chem. Phys.*, 18, 13457–13479, <https://doi.org/10.5194/acp-18-13457-2018>, 2018.
- Docherty, K. S., Wu, W., Lim, Y. B., and Ziemann, P. J.: Contributions of organic peroxides to secondary aerosol formed from reactions of monoterpenes with O₃, *Environ. Sci. Technol.*, 39, 4049–4059, <https://doi.org/10.1021/es050228s>, 2005.
- Elperin, T. and Fominykh, A.: Conjugate mass transfer during gas absorption by falling liquid droplet with internal circulation, *Atmos. Environ.*, 39, 4575–4582, <https://doi.org/10.1016/j.atmosenv.2005.04.005>, 2005.
- Epstein, S. A., Blair, S. L., and Nizkorodov, S. A.: Direct photolysis of α -pinene ozonolysis secondary organic aerosol: effect on particle mass and peroxide content, *Environ. Sci. Technol.*, 48, 11251–11258, <https://doi.org/10.1021/es502350u>, 2014.
- Gong, Y. W., Chen, Z. M., and Li, H.: The oxidation regime and SOA composition in limonene ozonolysis: roles of different

- double bonds, radicals, and water, *Atmos. Chem. Phys.*, 18, 15105–15123, <https://doi.org/10.5194/acp-18-15105-2018>, 2018.
- Gunn, R. and Kinzer, G. D.: The terminal velocity of fall for water droplets in stagnant air, *J. Meteorol.*, 6, 243–248, [https://doi.org/10.1175/1520-0469\(1949\)006<0243:TTVOFF>2.0.CO;2](https://doi.org/10.1175/1520-0469(1949)006<0243:TTVOFF>2.0.CO;2), 1949.
- Gurgueira, S. A., Lawrence, J., Coull, B., Murthy, G. G. K., and González-Flecha, B.: Rapid increases in the steady-state concentration of reactive oxygen species in the lungs and heart after particulate air pollution inhalation, *Environ. Health Perspect.*, 110, 749–755, <https://doi.org/10.1289/ehp.02110749>, 2002.
- Hasson, A. S. and Paulson, S. E.: An investigation of the relationship between gas-phase and aerosol-borne hydroperoxides in urban air, *J. Aerosol Sci.*, 34, 459–468, [https://doi.org/10.1016/S0021-8502\(03\)00002-8](https://doi.org/10.1016/S0021-8502(03)00002-8), 2003.
- He, S. Z., Chen, Z. M., Zhang, X., Zhao, Y., Huang, D. M., Zhao, J. N., Zhu, T., Hu, M., and Zeng, L. M.: Measurement of atmospheric hydrogen peroxide and organic peroxides in Beijing before and during the 2008 Olympic Games: chemical and physical factors influencing their concentrations, *J. Geophys. Res.-Atmos.*, 115, D17307, <https://doi.org/10.1029/2009JD013544>, 2010.
- Ho, K. F., Ho, S. S. H., Huang, R. J., Chuang, H. C., Cao, J. J., Han, Y. M., Lui, K. H., Ning, Z., Chuang, K. J., Cheng, T. J., Lee, S. C., Hu, D., Wang, B., and Zhang, R. J.: Chemical composition and bioreactivity of PM_{2.5} during 2013 haze events in China, *Atmos. Environ.*, 126, 162–170, <https://doi.org/10.1016/j.atmosenv.2015.11.055>, 2016.
- Hua, W., Chen, Z. M., Jie, C. Y., Kondo, Y., Hofzumahaus, A., Takegawa, N., Chang, C. C., Lu, K. D., Miyazaki, Y., Kita, K., Wang, H. L., Zhang, Y. H., and Hu, M.: Atmospheric hydrogen peroxide and organic hydroperoxides during PRIDE-PRD'06, China: their concentration, formation mechanism and contribution to secondary aerosols, *Atmos. Chem. Phys.*, 8, 6755–6773, <https://doi.org/10.5194/acp-8-6755-2008>, 2008.
- Huang, D. M. and Chen, Z. M.: Reinvestigation of the Henry's law constant for hydrogen peroxide with temperature and acidity variation, *J. Environ. Sci.*, 22, 570–574, [https://doi.org/10.1016/S1001-0742\(09\)60147-9](https://doi.org/10.1016/S1001-0742(09)60147-9), 2010.
- Huang, L. B., Zhao, Y., Li, H., and Chen, Z. M.: Kinetics of heterogeneous reaction of sulfur dioxide on authentic mineral dust: effects of relative humidity and hydrogen peroxide, *Environ. Sci. Technol.*, 49, 10797–10805, <https://doi.org/10.1021/acs.est.5b03930>, 2015.
- Kirkby, J., Duplissy, J., Sengupta, K., Frege, C., Gordon, H., Williamson, C., Heinritzi, M., Simon, M., Yan, C., Almeida, J., Tröstl, J., Nieminen, T., Ortega, I. K., Wagner, R., Adamov, A., Amorim, A., Bernhammer, A. K., Bianchi, F., Breitenlechner, M., Brilke, S., Chen, X. M., Craven, J., Dias, A., Ehrhart, S., Flagan, R. C., Franchin, A., Fuchs, C., Guida, R., Hakala, J., Hoyle, C. R., Jokinen, T., Junninen, H., Kangasluoma, J., Kim, J., Krapf, M., Kürten, A., Laaksonen, A., Lehtipalo, K., Makhmutov, V., Mathot, S., Molteni, U., Onnela, A., Peräkylä, O., Piel, F., Petäjä, T., Praplan, A. P., Pringle, K., Rap, A., Richards, N. A. D., Riipinen, I., Rissanen, M. P., Rondo, L., Sarnela, N., Schobesberger, S., Scott, C. E., Seinfeld, J. H., Sipil, M., Steiner, G., Stozhkov, Y., Stratmann, F., Tomé, A., Virtanen, A., Vogel, A. L., Wagner, A. C., Wagner, P. E., Weingartner, E., Wimmer, D., Winkler, P. M., Ye, P. L., Zhang, X., Hansel, A., Dommen, J., Donahue, N. M., Worsnop, D. R., Baltensperger, U., Kulmala, M., Carslaw, K. S., and Curtius, J.: Ion-induced nucleation of pure biogenic particles, *Nature*,

533, 521–526, <https://doi.org/10.1038/nature17953>, 2016.

555 Krapf, M., ~~El Haddad, I., Haddad, I. E.,~~ Bruns, E. A., Molteni, U., Daellenbach, K. R., Prévôt, A. S. H., Baltensperger, U., and Dommen, J.: Labile peroxides in secondary organic aerosol, *Chem*, 1, 603–616, <https://doi.org/10.1016/j.chempr.2016.09.007>, 2016.

~~Kuang, Y., Tao, J. C., Xu, W. Y., Yu, Y. L., Zhao, G., Shen, C. Y., Bian, Y. X., and Zhao, C. S.: Calculating ambient aerosol surface area concentrations using aerosol light scattering enhancement measurements, *Atmos. Environ.*, 216, 116919, <https://doi.org/10.1016/j.atmosenv.2019.116919>, 2019.~~

560 Kumar, S.: An Eulerian model for scavenging of pollutants by raindrops, *Atmos. Environ.*, 19, 769–778, [https://doi.org/10.1016/0004-6981\(85\)90065-4](https://doi.org/10.1016/0004-6981(85)90065-4), 1985.

Lee, M. H., Heikes, B. G., and O’Sullivan, D. W.: Hydrogen peroxide and organic hydroperoxide in the troposphere: a review, *Atmos. Environ.*, 34, 3475–3494, [https://doi.org/10.1016/S1352-2310\(99\)00432-X](https://doi.org/10.1016/S1352-2310(99)00432-X), 2000.

565 Levine, S. Z. and Schwartz, S. E.: In-cloud and below-cloud scavenging of nitric acid vapor, *Atmos. Environ.*, 16, 1725–1734, [https://doi.org/10.1016/0004-6981\(82\)90266-9](https://doi.org/10.1016/0004-6981(82)90266-9), 1982.

Li, H., Chen, Z. M., Huang, L. B., and Huang, D.: Organic peroxides’ gas-particle partitioning and rapid heterogeneous decomposition on secondary organic aerosol, *Atmos. Chem. Phys.*, 16, 1837–1848, [https://doi.org/10.5194/acp-16-1837-](https://doi.org/10.5194/acp-16-1837-2016) 2016, 2016.

570 ~~Li, K., Jacob, D. J., Liao, H., Zhu, J., Shah, V., Shen, L., Bates, K. H., Zhang, Q., and Zhai, S. X.: A two-pollutant strategy for improving ozone and particulate air quality in China, *Nat. Geosci.*, 12, 906–910, [https://doi.org/10.1038/s41561-019-0464-](https://doi.org/10.1038/s41561-019-0464-x)~~ x, 2019.

~~Li, T., Wang, Z., Wang, Y., Wu, C., Liang, Y., Xia, M., Yu, C., Yun, H., Wang, W., Wang, Y., Guo, J., Herrmann, H., and Wang, T.: Chemical characteristics of cloud water and the impacts on aerosol properties at a subtropical mountain site in Hong Kong, *Atmos. Chem. Phys. Discuss.*, <https://doi.org/10.5194/acp-2019-481>, in review, 2019.~~

575 ~~Li, T., Wang, Z., Wang, Y., Wu, C., Liang, Y., Xia, M., Yu, C., Yun, H., Wang, W., Wang, Y., Guo, J., Herrmann, H., and Wang, T.: Chemical characteristics of cloud water and the impacts on aerosol properties at a subtropical mountain site in Hong Kong SAR, *Atmos. Chem. Phys.*, 20, 391–407, <https://doi.org/10.5194/acp-20-391-2020>, 2020.~~

~~Liang, C. K., Pankow, J. F., Odum, J. R., and Seinfeld, J. H.: Gas/particle partitioning of semivolatile organic compounds to model inorganic, organic, and ambient smog aerosols, *Environ. Sci. Technol.*, 31, 3086–3092, <https://doi.org/10.1021/es9702529>, 1997.~~

580 Liang, H., Chen, Z. M., Huang, D., Zhao, Y., and Li, Z. Y.: Impacts of aerosols on the chemistry of atmospheric trace gases: a case study of peroxides and HO₂ radicals, *Atmos. Chem. Phys.*, 13, 11259–11276, [https://doi.org/10.5194/acp-13-11259-](https://doi.org/10.5194/acp-13-11259-2013) 2013, 2013.

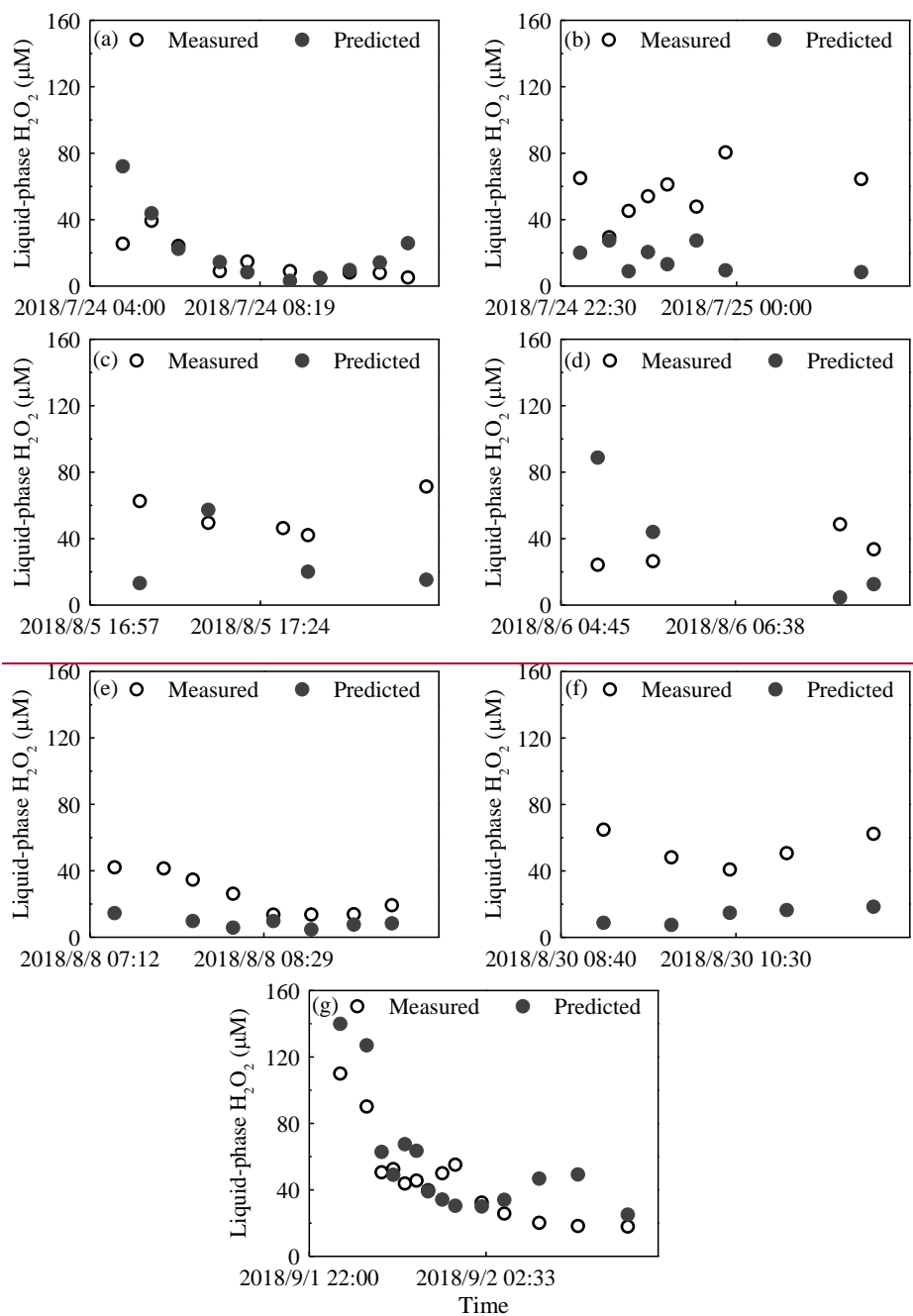
585 Lind, J. A., and Kok, G. L.: Henry’s law determinations for aqueous solutions of hydrogen peroxide, methylhydroperoxide, and peroxyacetic acid, *J. Geophys. Res.*, ~~Atmos.~~, 91, 7889–7895, <https://doi.org/10.1029/JD091iD07p07889>, 1986.

Liu, T. Y., Clegg, S. L., and Abbatt, J. P. D.: Fast oxidation of sulfur dioxide by hydrogen peroxide in deliquesced aerosol

- particles, Proc. Natl. Acad. Sci. U. S. A., 201916401, <https://doi.org/10.1073/pnas.1916401117>, 2020.
- Liu, Y. C., Wu, Z. J., Wang, Y., Xiao, Y., Gu, F. T., Zheng, J., Tan, T. Y., Shang, D. J., Wu, Y. S., Zeng, L. M., Hu, M., Bateman, A. P., and Martin, S. T.: Submicrometer particles are in the liquid state during heavy haze episodes in the urban atmosphere of Beijing, China, Environ. Sci. Technol. Lett., 4, 427–432, <https://doi.org/10.1021/acs.estlett.7b00352>, 2017.
- Ma, X. F., Tan, Z. F., Lu, K. D., Yang, X. P., Liu, Y. H., Li, S. L., Li, X., Chen, S. Y., Novelli, A., Cho, C. M., Zeng, L. M., Wahner, A., and Zhang, Y. H.: Winter photochemistry in Beijing: observation and model simulation of OH and HO₂ radicals at an urban site, Sci. Total Environ., 685, 85–95, <https://doi.org/10.1016/j.scitotenv.2019.05.329>, 2019.
- Maass, O. and Hiebert, P. G.: The properties of pure hydrogen peroxide. v. vapor pressure, J. Am. Chem. Soc., 46, 2693–2700, <https://doi.org/10.1021/ja01677a012>, 1924.
- Nozaki, K.: Iodometric method of analysis for organic peroxides, Ind. Eng. Chem., 18, 583–583, <https://doi.org/10.1021/i560157a020>, 1946.
- O’Sullivan, D. W., Lee, M., Noone, B. C., and Heikes, B. G.: Henry’s law constant determinations for hydrogen peroxide, methyl hydroperoxide, hydroxymethyl hydroperoxide, ethyl hydroperoxide, and peroxyacetic acid, J. Phys. Chem., 100, 3241–3247, <https://doi.org/10.1021/jp951168n>, 1996.
- Pankow, J. F.: An absorption model of gas-particle partitioning of organic compounds in the atmosphere, Atmos. Environ., 28, 185–188, [https://doi.org/10.1016/1352-2310\(94\)90093-0](https://doi.org/10.1016/1352-2310(94)90093-0), 1994.
- Penkett, S. A., Jones, B. M. R., Brich, K. A., and Eggleton, A. E. J.: The importance of atmospheric ozone and hydrogen peroxide in oxidising sulphur dioxide in cloud and rainwater, Atmos. Environ., 13, 123–137, <https://doi.org/10.1016/j.atmosenv.2007.10.065>, 1979.
- Pradhan, M., Kyriakou, G., Archibald, A. T., Papageorgiou, A. C., Kalberer, M., and Lambert, R. M.: Heterogeneous uptake of gaseous hydrogen peroxide by Gobi and Saharan dust aerosols: a potential missing sink for H₂O₂ in the troposphere, Atmos. Chem. Phys., 10, 7127–7136, <https://doi.org/10.5194/acp-10-7127-2010>, 2010.
- Pruppacher, H. R. and Klett, J. D.: Microphysics of clouds and precipitation, Kluwer Academic Publishers, Dordrecht, Holland, 1997.
- Qin, M. R., Chen, Z. M., Shen, H. Q., Li, H., Wu, H. H., and Wang, Y.: Impacts of heterogeneous reactions to atmospheric peroxides: observations and budget analysis study, Atmos. Environ., 183, 144–153, <https://doi.org/10.1016/j.atmosenv.2018.04.005>, 2018.
- Qiu, J., Ishizuka, S., Tonokura, K., Colussi, A. J., and Enami, S.: Water dramatically accelerates the decomposition of α -hydroxyalkyl-hydroperoxides in aerosol particles, J. Phys. Chem. Lett., 10, 5748–5755, <https://doi.org/10.1021/acs.jpcclett.9b01953>, 2019.
- Reeves, C. E. and Penkett, S. A.: Measurements of peroxides and what they tell us, Chem. Rev., 103, 5199–5218, <https://doi.org/10.1021/cr0205053>, 2003.
- Riva, M., Budisulistiorini, S. H., Zhang, Z. F., Gold, A., Thornton, J. A., Turpin, B. J., and Surratt, J. D.: Multiphase reactivity of gaseous hydroperoxide oligomers produced from isoprene ozonolysis in the presence of acidified aerosols, Atmos.

- Environ., 152, 314–322, <https://doi.org/10.1016/j.atmosenv.2016.12.040>, 2017.
- Romanias, M. N., El Zein, A., and Bedjanian, Y.: Heterogeneous interaction of H₂O₂ with TiO₂ surface under dark and UV light irradiation conditions, *J. Phys. Chem. A*, 116, 8191–8200, <https://doi.org/10.1021/jp305366v>, 2012.
- 625 Romanias, M. N., El Zein, A., and Bedjanian, Y.: Uptake of hydrogen peroxide on the surface of Al₂O₃ and Fe₂O₃, *Atmos. Environ.*, 77, 1–8, <https://doi.org/10.1016/j.atmosenv.2013.04.065>, 2013.
- Sander, S. P., Abbatt, J., Barker, J. R., Burkholder, J. B., Friedl, R. R., Golden, D. M., Huie, R. E., Kolb, C. E., Kurylo, M. J., Moortgat, G. K., Orkin, V. L., and Wine, P. H.: Chemical kinetics and photochemical data for use in atmospheric studies, Evaluation No. 17, JPL Publication 10-6, Jet Propulsion Laboratory, Pasadena, <http://jpldataeval.jpl.nasa.gov> (last access: 630 [19 March 2020](#)), 2011.
- Seinfeld, J. H. and Pandis S. N.: Atmospheric chemistry and physics: from air pollution to climate change, A Wiley-Interscience Publication, New Jersey, the United States of America, 2006.
- Shang, B., Zhou, Y. Q., Liu, J. C., and Huang, Y. M.: Comparing vertical structure of precipitation cloud and non-precipitation cloud using Cloudsat, *J. Appl. Meteorol. ClimSci.*, 23, 1–9, <https://doi.org/10.3969/j.issn.1001-7313.2012.01.001>, 2012.
- 635 Shao, P. Y., Tian, H. Z., Sun, Y. J., Liu, H. J., Wu, B. B., Liu, S. H., Liu, X. Y., Wu, Y. M., Liang, W. Z., Wang, Y., Gao, J. J., Xue, Y. F., Bai, X. X., Liu, W., Lin, S. M., and Hu, G. Z.: Characterizing remarkable changes of severe haze events and chemical compositions in multi-size airborne particles (PM₁, PM_{2.5} and PM₁₀) from January 2013 to 2016–2017 winter in Beijing, China, *Atmos. Environ.*, 189, 133–144, <https://doi.org/10.1016/j.atmosenv.2018.06.038>, 2018.
- Shen, H., Barakat, A. I., and Anastasio, C.: Generation of hydrogen peroxide from San Joaquin Valley particles in a cell-free 640 solution, *Atmos. Chem. Phys.*, 11, 753–765, <https://doi.org/10.5194/acp-11-753-2011>, 2011.
- Shen, H. Q., Chen, Z. M., Li, H., Qian, X., Qin, X., and Shi, W. X.: Gas-particle partitioning of carbonyl compounds in the ambient atmosphere, *Environ. Sci. Technol.*, 52, 10997–11006, <https://doi.org/10.1021/acs.est.8b01882>, 2018.
- Shiraiwa, M., Ammann, M., Koop, T., and Pöschl, U.: Gas uptake and chemical aging of semisolid organic aerosol particles, *Proc. Natl. Acad. Sci. U. S. A.*, 108, 11003–11008, <https://doi.org/10.1073/pnas.1103045108>, 2011.
- 645 Slade, J. H. and Knopf, D. A.: Multiphase OH oxidation kinetics of organic aerosol: the role of particle phase state and relative humidity, *Geophys. Res. Lett.*, 41, 5297–5306, <https://doi.org/10.1002/2014GL060582>, 2015.
- Stein, A. F. and Saylor, R. D.: Sensitivities of sulfate aerosol formation and oxidation pathways on the chemical mechanism employed in simulations, *Atmos. Chem. Phys.*, 12, 8567–8574, <https://doi.org/10.5194/acp-12-8567-2012>, 2012.
- Tong, H., Arangio, A. M., Lakey, P. S. J., Berkemeier, T., Liu, F., Kampf, C. J., Brune, W. H., Pöschl, U., and Shiraiwa, M.: 650 Hydroxyl radicals from secondary organic aerosol decomposition in water, *Atmos. Chem. Phys.*, 16, 1761–1771, <https://doi.org/10.5194/acp-16-1761-2016>, 2016.
- Wang, Y., Chen, Z. M., Wu, Q. Q., Liang, H., Huang, L. B., Li, H., Lu, K. D., Wu, Y. S., Dong, H. B., Zeng, L. M., and Zhang, Y. H.: Observation of atmospheric peroxides during Wangdu Campaign 2014 at a rural site in the North China Plain, *Atmos. Chem. Phys.*, 16, 10985–11000, <https://doi.org/10.5194/acp-16-10985-2016>, 2016.
- 655 Wang, Y., Kim, H., and Paulson, S. E.: Hydrogen peroxide generation from α - and β -pinene and toluene secondary organic

- aerosols, *Atmos. Environ.*, 45, 3149–3156, <https://doi.org/10.1016/j.atmosenv.2011.02.060>, 2011.
- Williams, B. J., Goldstein, A. H., Kreisberg, N. M., and Hering, S. V.: In situ measurements of gas/particle-phase transitions for atmospheric semivolatile organic compounds, *Proc. Natl. Acad. Sci. U. S. A.*, 107, 6676–6681, <https://doi.org/10.1073/pnas.0911858107>, 2010.
- 660 Wu, Q. Q., Huang, L. B., Liang, H., Zhao, Y., Huang, D., and Chen, Z. M.: Heterogeneous reaction of peroxyacetic acid and hydrogen peroxide on ambient aerosol particles under dry and humid conditions: kinetics, mechanism and implications, *Atmos. Chem. Phys.*, 15, 6851–6866, <https://doi.org/10.5194/acp-15-6851-2015>, 2015.
- Xie, M. J., Hannigan, M. P., and Barsanti, K. C.: Gas/particle partitioning of n-alkanes, PAHs and oxygenated PAHs in urban Denver, *Atmos. Environ.*, 95, 355–362, <https://doi.org/10.1016/j.atmosenv.2014.06.056>, 2014.
- 665 Xu, Z. F., Tang, Y., and Ji, J. P.: Chemical and strontium isotope characterization of rainwater in Beijing during the 2008 Olympic year, *Atmos. Res.*, 107, 115–125, <https://doi.org/10.1016/j.atmosres.2012.01.002>, 2012.
- Ye, C., Liu, P. F., Ma, Z. B., Xue, C. Y., Zhang, C. L., Zhang, Y. Y., Liu, J. F., Liu, C. T., Sun, X., and Mu, Y. J.: High H₂O₂ concentrations observed during haze periods during the winter in Beijing: importance of H₂O₂ oxidation in sulfate formation, *Environ. Sci. Technol. Lett.*, 5, 757–763, <https://doi.org/10.1021/acs.estlett.8b00579>, 2018.
- 670 Zhao, R., Kenseth, C. M., Huang, Y., Dalleska, N. F., and Seinfeld, J. H.: Iodometry-assisted liquid chromatography electrospray ionization mass spectrometry for analysis of organic peroxides: an application to atmospheric secondary organic aerosol, *Environ. Sci. Technol.*, 52, 2108–2117, <https://doi.org/10.1021/acs.est.7b04863>, 2018.
- Zhao, Y., Chen, Z. M., Shen, X. L., and Huang, D.: Heterogeneous reactions of gaseous hydrogen peroxide on pristine and acidic gas-processed calcium carbonate particles: effects of relative humidity and surface coverage of coating, *Atmos. Environ.*, 67, 63–72, <https://doi.org/10.1016/j.atmosenv.2012.10.055>, 2013.
- 675 Zhao, Y., Chen, Z. M., Shen, X. L., and Zhang, X.: Kinetics and mechanisms of heterogeneous reaction of gaseous hydrogen peroxide on mineral oxide particles, *Environ. Sci. Technol.*, 45, 3317–3324, <https://doi.org/10.1021/es104107c>, 2011.
- Zhou, X. L., Davis, A. J., Kieber, D. J., Keene, W. C., Maben, J. R., Maring, H., Dahl, E. E., Izaguirre, M. A., Sander, R., and Smoydzyn, L.: Photochemical production of hydroxyl radical and hydroperoxides in water extracts of nascent marine aerosols produced by bursting bubbles from Sargasso seawater, *Geophys. Res. Lett.*, 35, L20803, <https://doi.org/10.1029/2008GL035418>, 2008.



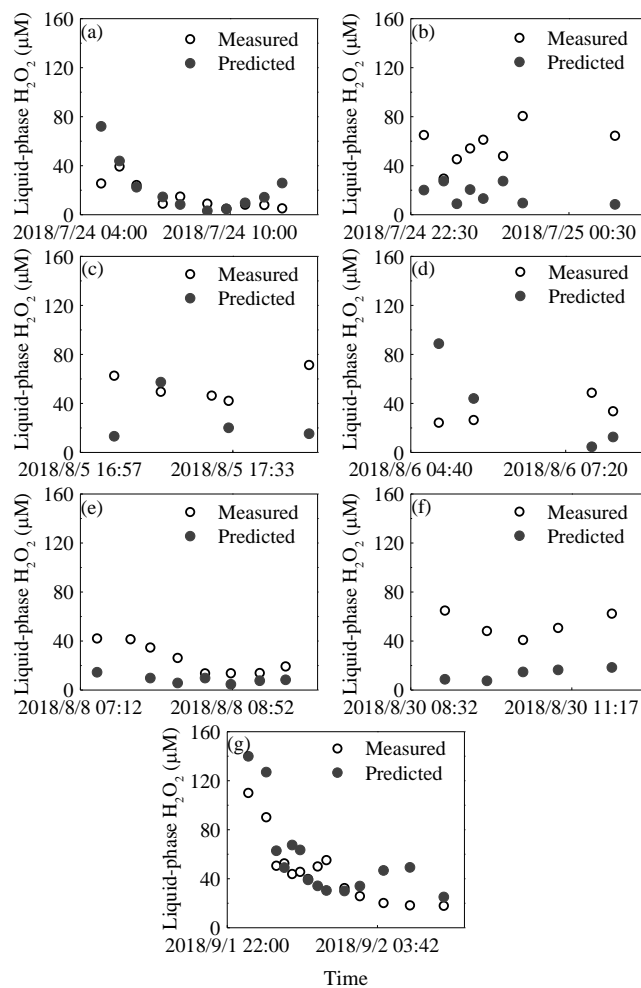


Figure 1: Time profiles of measured and predicted concentrations of H_2O_2 from seven rain episodes. The seven rainfall events are listed in chronological order: (a) 24 July, (b) 25 July, (c) 5 August, (d) 6 August, (e) 8 August, (f) 30 August, and (g) 2 September.

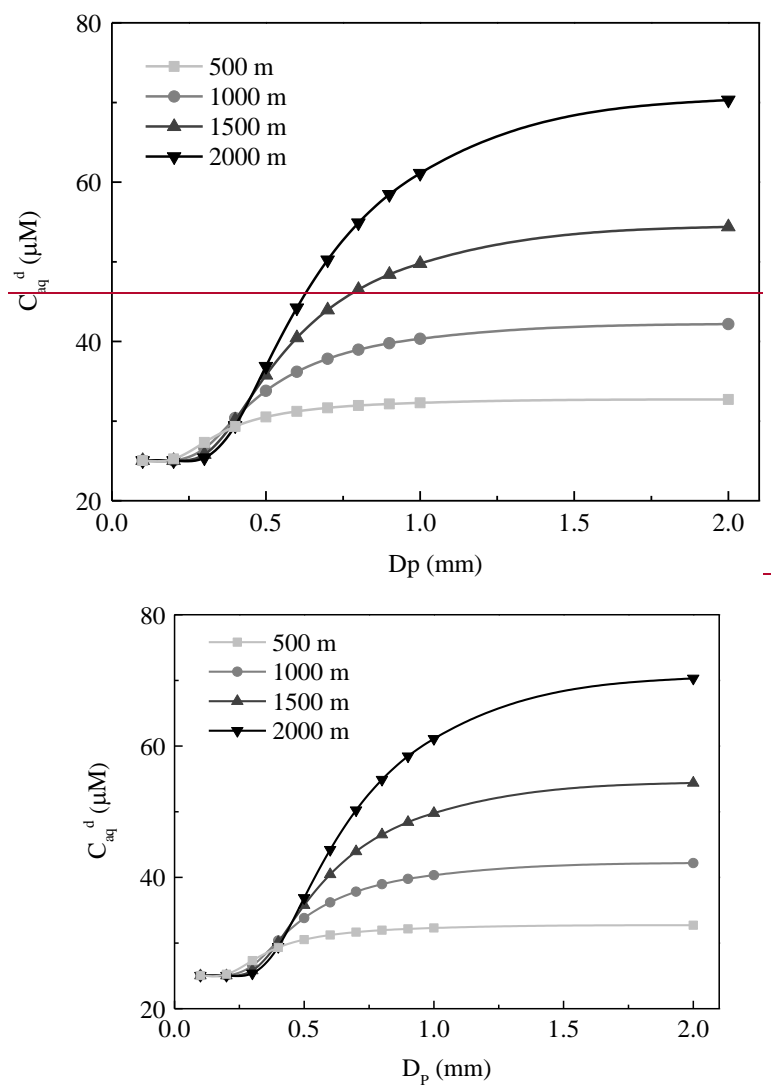


Figure 2: The dependence of the concentration of H_2O_2 in the ground raindrops (C^d_{aq}) on the diameter of the raindrops (D_p). The light grey, grey, dark grey, and black lines denote fall distances of 500 m, 1000 m, 1500 m, and 2000 m, respectively.

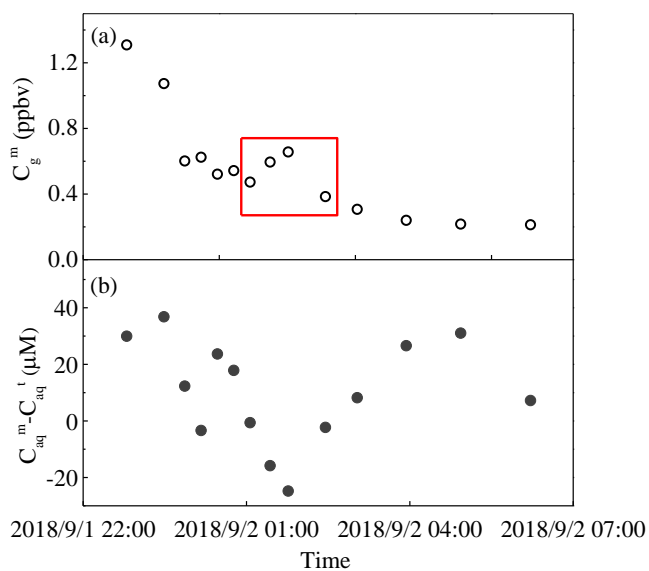
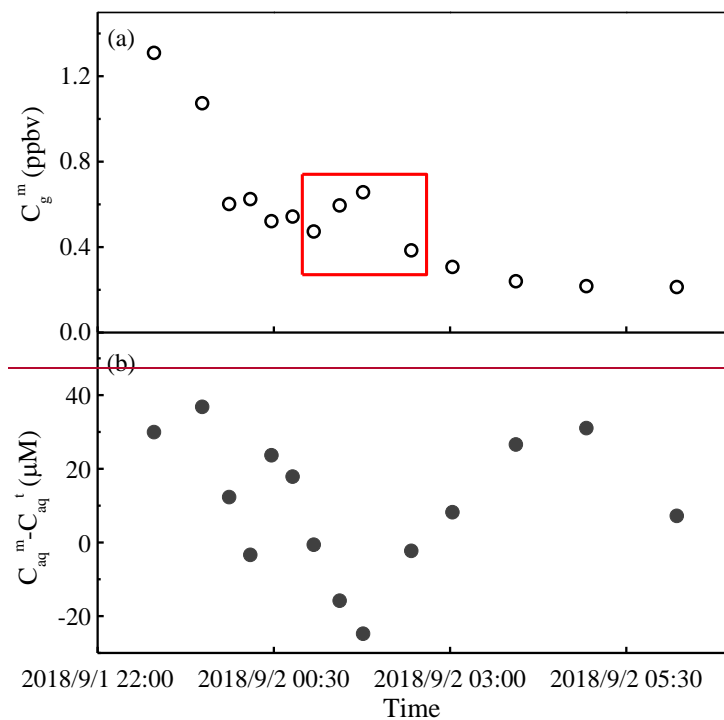


Figure 3: The measured and predicted H_2O_2 levels in a rain event on 1–2 September 2018. (a) Measured gas-phase H_2O_2 (C_g^m). (b) The difference between measured (C_{aq}^m) and theoretical (C_{aq}^t) levels of H_2O_2 in the liquid phase. The red box indicates a sudden rise in gas-phase H_2O_2 .

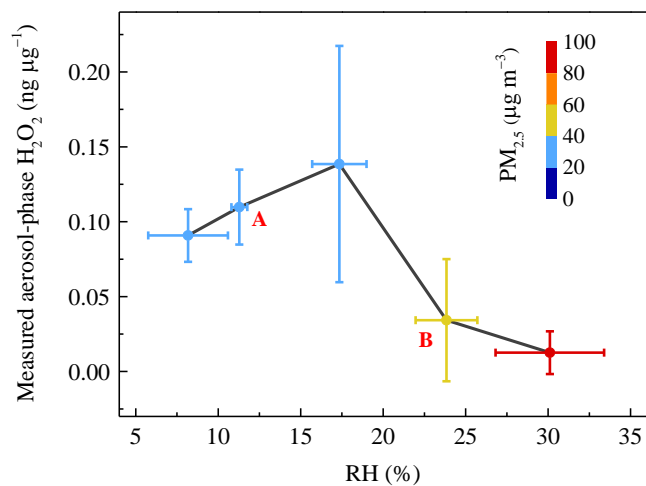
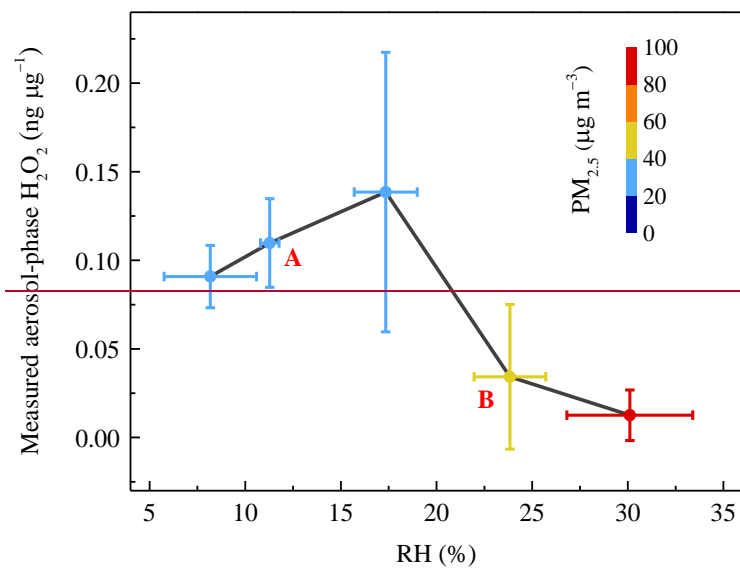


Figure 4: The relationship between measured aerosol-phase H_2O_2 level and relative humidity (RH). Coloured circles denote the mass concentration of $PM_{2.5}$. The vertical error bars represent the standard deviations of aerosol-phase H_2O_2 concentration in every RH range bin.

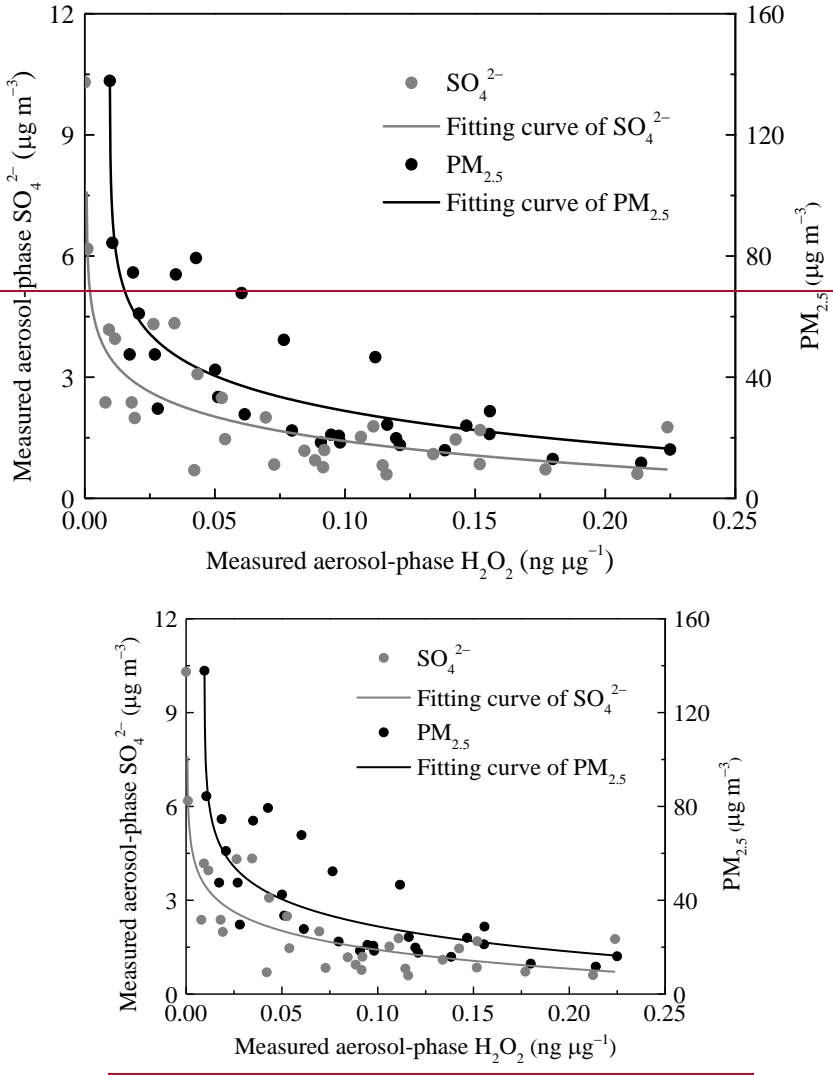
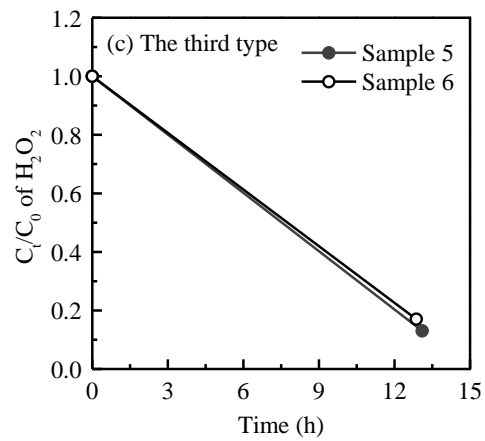
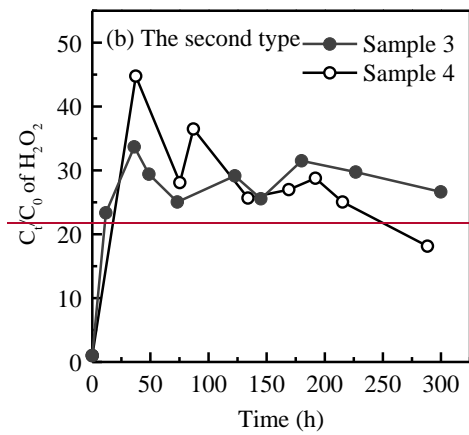
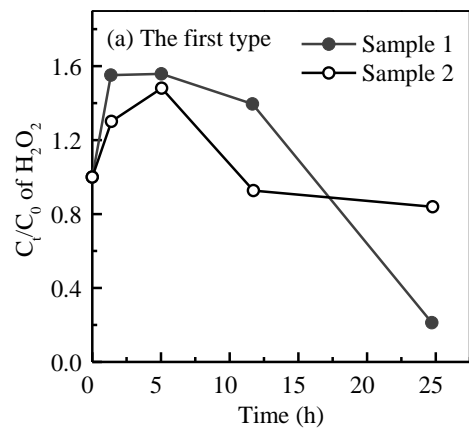


Figure 5: The negative dependence of the measured concentrations of aerosol-phase SO₄²⁻ and PM_{2.5} on H₂O₂. The grey and black lines are the logarithmic fits for SO₄²⁻ level in aerosols and the PM_{2.5} mass concentration, respectively.



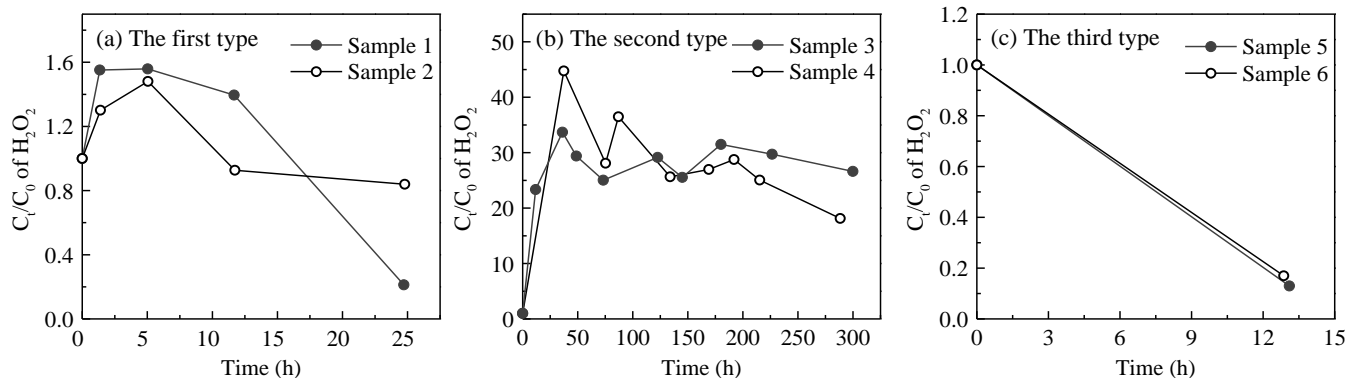


Figure 6: Time profiles of aerosol-phase H_2O_2 evolution in the extracted solution. (a) The first type: samples 1 and 2 were collected on 29 December 2018. (b) The second type: samples 3 and 4 were gathered on 31 December 2018–1 January 2019. (c) The third type: samples 5 and 6 were collected on 2 January 2019. C_t and C_0 denote molar concentrations of H_2O_2 in the extracted solution at time= t and time= 0 .

720

Table 1: Calculating the level of H₂O₂ in the ground raindrops (C_{aq}^d) with different diameters (D_P) from a height of 1000 m^a.

Parameters	D_P (mm)			
	0.1	0.5	1.0	2.0
u (m s ⁻¹) ^b	0.27	2.06	4.03	6.49
k_g (cm s ⁻¹) ^c	51.42	25.00	21.09	17.45
C_{aq}^d (μM)	25.03	33.81	40.34	42.18

^a These parameters are calculated based on equations in Gunn and Kinzer (1949), Levine and Schwartz (1982), Kumar (1985), and Seinfeld and Pandis (2006).

^b u is the terminal fall velocity of a raindrop.

^c k_g is the mass transfer coefficient of H₂O₂ in the gas phase.

Table 2: Estimates of the level of H₂O₂ in cloud water (C_{aq}^c) and the surrounding atmosphere (C_g^c) at different fall distances with a raindrop diameter of 1.0 mm.

Parameters	500 m	1000 m	1500 m	2000 m
T_S^c (K) ^a	295	292	289	286
H_A^t (M atm ⁻¹)	1.1×10^5	1.4×10^5	1.9×10^5	2.5×10^5
C_{aq}^c (μM)	45.64	47.27	49.04	50.95
C_g^c (ppbv)	0.41	0.33	0.26	0.21

^a T_S^c is the temperature in cloud water.

Table 3: ~~Calculating Comparison between~~ the theoretical heterogeneous uptake rate of H₂O₂ on aerosols ($d[X]_p^{t,h}/dt$) ~~and the measured aerosol phase H₂O₂ level ($[X]_p^{me}$)~~^a.

Parameters	T_W (K)	RH (%)	γ - ^b	$A_{es}S_{aw}$ (cm ²) ^c	$[X]_g$ (molecules m ⁻³) ^d	$d[X]_p^{t,h}/dt$ (ng μ g ⁻¹ h ⁻¹)
Averages	270	17.89	1.54×10^{-4}	9.00 46	6.65 6.54 $\times 10^{14}$	0.049 0.02

^a These parameters are calculated based on Wu et al. (2015).

^b γ is the heterogeneous uptake coefficient, dimensionless.

^c $A_{es}S_{aw}$ is the ~~effective reactions~~surface area of aerosols, quoted from Kuang et al. (2019).

^d $[X]_g$ is the concentration of gas-phase H₂O₂.

735 **Table 4: Comparison of the H₂O₂ evolution parameters in the extracted solution among the three types.**

Parameters	First type	Second type	Third type
Peak time (h)	5	40	–
Decomposition rate of organic peroxides to H₂O₂ (ng µg⁻¹)	0.14	3.65	=
Decomposition rate of organic peroxides to H₂O₂ (ng µg⁻¹ h⁻¹)	0.01	0.10	–
<i>C_{max}/C₀</i> of H ₂ O ₂ (µM/µM)	1.52	39.22	1.00
TPOs/H ₂ O ₂ (µM/µM)	5.25	40.06	47.59
Ratio of decomposable organic peroxides (%)	29	98	0
Possible organic peroxides	PCAs^a, α-HAHPs^b	PCAs, α-HAHPs	ROOR ^c

^a~~PCAs denote peroxyacetic acids, e.g., peroxyacetic acid, PAA; peroxyformic acid, PFA.~~
^b~~α-HAHPs denote α-hydroxyalkyl hydroperoxides, e.g., hydroxymethyl hydroperoxide, HMHP.~~
^c~~ROOR denote peroxide esters.~~